Elsevier Editorial System(tm) for International Journal for Parasitology
Manuscript Draft

Manuscript Number: IJPara09_064R1

Title: "5-Me-6-BIO targeting the leishmanial GSK-3 short form affects cell-cycle progression and induces apoptosis-like death: exploitation of GSK-3 for treating leishmaniasis"

Article Type: Full Length Article

Section/Category: Medical and Veterinary Parasitology

Keywords: L. donovani glycogen synthase kinase-3 short; 5-Me-6-BIO; 6-BIO; indirubins; apoptosis-like death; drug target

Corresponding Author: Dr Ketty Soteriadou,

Corresponding Author's Institution: Hellenic Pasteur Institute

First Author: Evangelia Xingi

Order of Authors: Evangelia Xingi; Despina Smirlis ; Vassilios Myrianthopoulos; Prokopios Magiatis ; Karen Grant; Laurent Meijer ; Emmanuel Mikros; Alexios-Leandros Skaltsounis; Ketty Soteriadou

Manuscript Region of Origin: GREECE

Abstract: Indirubins known to target mammalian cyclin-dependent kinases (CDKs) and glycogen synthase kinase (GSK-3) were tested for their antileishmanial activity. 6-Br-indirubin-3'-oxime (6-BIO), 6-Br-indirubin-3'acetoxime and 6-Br-5methylindirubin-3'oxime (5-Me-6-BIO) were the most potent inhibitors of L. donovani promastigote and amastigote growth (IC50 values ≤ 1.2 μM). Since the 6-Br substitution on the indirubin backbone greatly enhances the selectivity for mammalian GSK-3 over CDKs, we identified the leishmanial GSK-3 homologues, a short (LdGSK-3s) and a long one, focusing on LdGSK-3s which is closer to human GSK-3β for further studies. Kinase

assays showed that 5-Me-6-BIO inhibited LdGSK-3s more potently than CRK3 (the CDK1 homologue in Leishmania), while 6-BIO was more selective for CRK3. Promastigotes treated with 5-Me-6-BIO accumulated in the S and G2/M cell-cycle phases and underwent apoptosis-like death. Interestingly, these phenotypes were completely reversed in parasites over-expressing LdGSK-3s. This finding strongly supports that LdGSK-3s is a) the intracellular target of 5-Me-6-BIO and b) involved in cell-cycle control and in pathways leading to apoptosis-like death. 6-BIO treatment induced a G2/M arrest, consistent with inhibition of CRK3, and apoptosis-like death. These effects were partially reversed in parasites over-expressing LdGSK-3s suggesting that in vivo 6-BIO may also target LdGSK-3s. Molecular docking of 5-Me-6-BIO in CRK3 and 6-BIO in human GSK-3β and LdGSK-3s active sites predict the existence of functional/structural differences that are sufficient to explain the observed difference in their affinity. In conclusion, LdGSK-3s is validated as a potential drug target in Leishmania and could be exploited for the development of selective indirubin-based leishmanicidals.

AUTHOR AGREEMENT FORM

Manuscript title: "5-Me-6-BIO targeting the leishmanial GSK-3 short form affects cell-cycle progression and induces apoptosis-like death: exploitation of GSK-3 for treating leishmaniasis"

Authors: Evangelia Xingi, Despina Smirlis , Vassilios Myrianthopoulos , Prokopios Magiatis, Karen M. Grant, Laurent Meijer, Emmanuel Mikros, Alexios-Leandros Skaltsounis and Ketty Soteriadou

We, the undersigned, acknowledge that we have read the above manuscript and accept responsibility for its contents. We confirm this manuscript has not been published previously and if accepted in the *International Journal for Parasitology* will not be published elsewhere without the approval of the Editor-in-Chief. We also confirm there are no financial or other relationships that might lead to a conflict of interest.

[If a financial or other relationship exists that might lead to a conflict of interest, please provide that information here.]

[If this letter is being submitted at revision and if there have been any changes in authors added to/deleted from the paper or if the order of author citation has changed since the original submission, please include a statement acknowledging those changes, before each author (including authors deleted from the paper) signs this letter.]

Signatures of authors in order of citation: Evangelia Xingi, Despina Smirlis , Vassilios Myrianthopoulos , Prokopios Magiatis, Laurent Meijer, Emmanuel Mikros, Alexios-Leandros Skaltsounis, Ketty Soteriadou, Karen M. Grant,

*** Cover Letter**

Ms. Ref. No.: IJPara09_064
Title: 5-Me-6-BIO targeting the leishmanial GSK-3<beta> affects cell-cycle progression and induces apoptosis-like death: exploitation of GSK-3<beta> for treating leishmaniasis

Dear Editor,

First, I would like to thank you for giving us the opportunity to reconsider your decision on our submitted manuscript. Please note that in the title we have changed GSK-3β to GSK-3 short form. We have addressed most if not all of the comments raised by the reviewers and explained how we dealt with point by point in the "Response to Reviews".

We hope that the revised version of our MS covers the reviewers concerns.

Yours sincerely,

Ketty Soteriadou, PhD
Research Director
Laboratory of Molecular Parasitology
Hellenic Pasteur Institute, Bas. Sofias 127, 11521
tel: +30-2106478841
email: ksoteriadou@pasteur.gr

"Response to Reviews"

Ms. Ref. No.: IJPara09_064
Title: 5-Me-6-BIO targeting the leishmanial GSK-3<beta> affects cell-cycle progression and induces apoptosis-like death: exploitation of GSK-3<beta> for treating leishmaniasis

Reviewer #1: General Remarks:

In this study, the authors evaluated the antileishmanial activity of sixteen indirubin compounds known to target mammalian cyclin-dependent kinases and glycogen synthase kinase (GSK-3). Both developmental forms of Leishmania donovani life cycle were tested and three 6-bromo substituted indirubins (e.g. 5-Me-6-BIO, 6-BIO and 6-BIA) were found to be more potent inhibitors of L. donovani promastigotes but interestingly also of intracellular amastigotes. Experimental evidence provided here strongly supports that the L. donovani LdGSK-3beta homolog is the main intracellular target of 5-Me-6-BIO and suggests a potential role of GSK-3beta in cell cycle progression and in apoptotic-like death. The data also indicate that 6-BIO targets less efficiently LdGSK-3beta but binds with much higher affinity to the Leishmania CRK3 kinase inducing also G2/M arrest and apoptosis-like death. Removal of the inhibitor or overexpression of LdGSK-3beta, but not of a kinase dead mutant, by Leishmania completely reverts the inhibitory cellular effects induced by 5-Me-6-BIO but only a partial reversion was seen with 6-BIO treatment, further supporting the targeting specificity of 5-Me-6-BIO for LdGSK-3beta. Although, the validity of GSK-3 as a potential drug target has been recently evaluated in T. brucei and few indirubin compounds have been used previously to target cyclin-dependent kinases in L. mexicana, this study extends beyond these previous investigations by evaluating more indirubin compounds on different cell-cycle forms of L. donovani and by providing sufficient insight on the cellular targets and their binding specificity as well as on their potential biological function. The conclusions here are well supported by a large set of experiments and the work is interesting and generally well conducted.
More efforts toward the development of novel antileishmanial drugs should generally be devoted, and this study is relevant and in line with such initiatives.

Specific remarks:

1- Although the effect of 5-Me-6-BIO on LdGSK-3beta is clearly specific and implies that the LdGSK-3beta is the main target of 5-Me-6-BIO, it is surprising however, that only a 2-fold increase in the expression of LdGSK-3beta kinase in the Leishmania overexpressor was able to revert completely the inhibitory cellular effects (e.g. of growth inhibition, cell-cycle progression and apoptosis-like death) induced by 5-Me-6-BIO. Is that possible that the HA-tagged version of GSK-3beta has a higher affinity for 5-Me-6-BIO than the WT enzyme or that may be this tagged protein undergoes a different phosphorylation or autophosphorylation pattern resulting in changes of its binding affinity to the inhibitors? Determining the inhibition (IC50) of this tagged protein kinase

activity by 5-Me-6-BIO will probably answers part of this question. The authors should discuss this interesting but intriguing result.

May be it was not clearly stated but as described in the Material and Methods as well as in the Results Sections kinase assays were performed with the $(His)_6$-tagged LdGSK-3s purified from LdGSK-3s over-expressing transfectants. Therefore the calculated IC50 is that of the His-tagged LdGSK-3s (0.09 µM). We cannot measure the IC50 of the wild type kinase since we have not purified the wild type kinase. However, the finding that wild type promastigotes as well as sat-transfectants after 72h of treatment were inhibited by 5-Me-6-BIO with an IC50 of 1.2±0.2 µM and 1.2±0.1 µM respectively while the respective IC_{50} for the LdGSK-3s over-expressing transfectants, where there is a 2-fold increase in LdGSK-3s, was approximately 2-fold higher IC_{50} 2.8±0.2 µM (Fig. 5A,B) suggest that the wild-type kinase should be inhibited by 5-Me-6-BIO with an IC50 value comparable with that of the His-tagged LdGSK-3s. We have commented on this in the Discussion Section, as suggested by the reviewer (lines 688-689).

2- Given that LdGSK-3beta expression and subcellular localization are different between L. donovani promastigotes and amastigotes, it is somewhat surprising that the IC50, especially for 5-Me-6-BIO, is the same for promastigotes and intracellular amastigotes. Could the authors comment on that?

We believe that the fact that the IC50 values against 5-Me-6-BIO are approximately the same between the two stages may be explained by a higher activity of the kinase in amastigotes stage than in promastigotes which may be associated with the different pH and temperature conditions. Also we cannot exclude that 5-Me-6-BIO may also target other kinase in this stage.
We have included a comment on this in the Discussion section (lines 656-658)

3- There are two GSK-3 isoforms (alpha and beta) in L. donovani. The authors have only investigated the LdGSK-3beta isoform. Did overexpression studies done with the GSK-3alpha isoform revert also the phenotype induced by 5-Me-6-BIO? It will be important to assess in future studies whether the GSK3-alpha isoform is also inhibited by the selected indirubin compounds to further validate GSK-3 as a potential drug target.

Please note that we have renamed the studied homologue from GSK-3β to GSK-3 short (see reply to comment 1, reviewer 2).
We have studied only the LdGSK-3short isoform, because it is almost identical in different Leishmania species and is closer to both the mammalian GSK-3 isoforms. Indeed future studies focusing on GSK3 long isoform and its inhibition by the selected indirubin compounds will further validate GSK-3 as a potential drug target.

4- The manuscript is overall well written but is too long and needs to be reduced significantly in length. For example, reorganizing the different subsections and merging

some of them should shorten the Materials and methods section. The Results section needs also to be shortened, especially the last section 3.8. It will also be preferable to integrate the 6-BIO data (section 3.7) together with the 5-Me-6-BIO data, as most of the observed phenotype with either inhibitor is quite similar. This will also save some space.

Following the suggestions of the reviewer we have merged in the Materials and methods 2.4 (Analysis of indirubin-treated promastigotes by flow cytometry) with 2.6 (Double staining with Annexin V and PI) and 2.13 (Expression of Leishmania Histone H1) with 2.14 (Kinase assays). This has shortened this section.
We also have integrated section 3.7 of the initial submission (G2/M phase arrest and induction of apoptosis-like death in 6-BIO-treated L. donovani promastigotes: LdGSK-3s over-expression counteracts 6-BIO induced cellular effects) with sections 3.5 and 3.6 . Thus the new sections 3.5 and 3.6 are shorter.
We also have shortened section 3.8 (Structure Activity Relationships studies of indirubin-leishmanial kinases interactions using molecular simulations) that is 3.7 in the revised manuscript. Some data on 3.7 are provided as supplementary.

5- 6-BIO has a much higher binding affinity (IC50=0.005uM) for the human GSK-3beta than for the Leishmania enzyme (IC50=0.15uM) but it has a stronger affinity for the Leishmania CRK3 (IC50=0.02 uM). On the other hand, 5-Me-6-BIO has a high affinity (IC50=0.09uM) for the LdGSK-3beta but there is no mention on its binding affinity for the human ortholog.
The data generated from the molecular docking experiments in section 3.8 should be better discussed in the context of the binding affinities of these inhibitors to the Leishmania kinase targets vs. the corresponding human targets and what it could be done to improve or to reverse some of these binding affinities in order to increase parasite killing while reducing toxicity to human cells.

We have included this omission concerning the activity of 5-Me-6-BIO for its human ortholog (lines 577-580). Also possible ways for the improvement of the affinities of indirubins towards parasite kinases have been incorporated in the Results (3.7 last paragraph lines 619-625) as suggested by the reviewer.

Minor points:

6- Figure 1 might be included as a supplemental material.

Figure 1 is provided as supplemental material, as suggested by the reviewer.

7- The Alamar blue assay, although it constitutes an improvement over other staining assays is not very quantitative for measuring intramacrophage Leishmania growth. Therefore, more quantitative assays that make use of reporter genes should eventually be used in the future to better evaluate the activity of indirubin compounds on intracellular amastigotes in vivo.

We discuss the disadvantages of Alamar blue assay for measuring the growth of intracellular amastigotes compared to the use of reporter genes in the Discussion section of the revised manuscript (line 634-637).

8-This reviewer would like to stress the attention on the possibility that some of the indirubin compounds targeting specifically GSK-3 might have an effect on the host immune responses against the parasite, hence altering parasite growth inside macrophages (see the paper by Ohtani M, et al., Blood 2008).

We would like to note that in the context of this study we have not used activated macrophages and therefore LPS-induced phosporylation of GSK-3 which in turn regulates IL-12 production is not applicable. However, since this is an important issue we have briefly stated in the Discussion of the revised manuscript that indirubins (GSK-3 inhibitors) may affect host immune responses (lines 724-726)

Reviewer #2:
This paper describes the effects of indirubin derivatives on Leishmania. The compounds causes cell cycle defects and apoptosis-like cell death. Based on the fact that this family of compounds target GSK3 in mammalian cells, the authors focus subsequent work on one of the GSK3-like enzymes, LdGSK3beta (the reasons given to select one rather than the other -"most well-studied mammalian isoform" and "almost identical in different Leishmania species"- are not compelling). The central finding is that over-expression of LdGSK3beta renders parasite more resistant to the inhibitor, suggesting the enzyme is a major target.
The topic is clearly of interest. My main concern with the paper is its length: lack of concision causes a dilution of the central points. The text should be shortened significantly (several sections, e.g. the data on the Paullones, might be included as supplementary information), so as to present the main findings in a more incisive way.

We have shortened the revised manuscript by ~ 20% and data on additional structurally divergent inhibitors (e.g. Paullones) has been provided as supplemental.

There are also additional issues that should be addressed before the manuscript becomes suitable for publication.

Major points :

1. Phylogeny of the Leishmania GSK3 enzymes. The authors rather summarily say (line 406) that LGSK3a and GSK3b are "equivalent" to mammalian GSK3a and GSK3b. What does this mean? A simple phylogenetic tree of alpha and beta orthologues from several species is required to support the statement. The two GSK3-like proteins were identified in the Parsons et al., study of the kinome of trypanosmatids, which should be cited here (Comparative analysis of the kinomes of three pathogenic trypanosomatids: Leishmania

major, Trypanosoma brucei and Trypanosoma cruzi. Parsons M, Worthey EA, Ward PN, Mottram JC. BMC Genomics. 2005 Sep 15;6:127).

The phylogenetic tree of alpha and beta orthologues from several species is provided for the reviewer but it is not included in the submitted revised version. For generating the tree GSK-3 protein sequences from different species were aligned and for the analysis PHYLIP package was used. For tree construction, we used either the neighbor-joining (NJ) method with at least 100 bootstrap samples, or the heuristic approximation of the maximum likelihood (ML) method which produced trees with the same topology. The Leishmania GSK-3 forms group with the T. brucei and T. cruzi homologues and are close to the S. cerevisiae GSK-3β proteins. Oddly both the Leishmania GSK-3 forms seem to have the same distance from the mammalian GSK-3 forms. This could be explained by the fact that Leishmania GSK-3 long is characterized by several long amino-acid stretches which do not correspond to sequences from GSK-3 molecules from the other species and force the alignment algorithms to introduce a lot of gaps. The gaps in the multiple alignments are ignored by the tree construction algorithms, thus producing a tree in which the differences between the two Leishmania GSK-3 forms are not well represented.

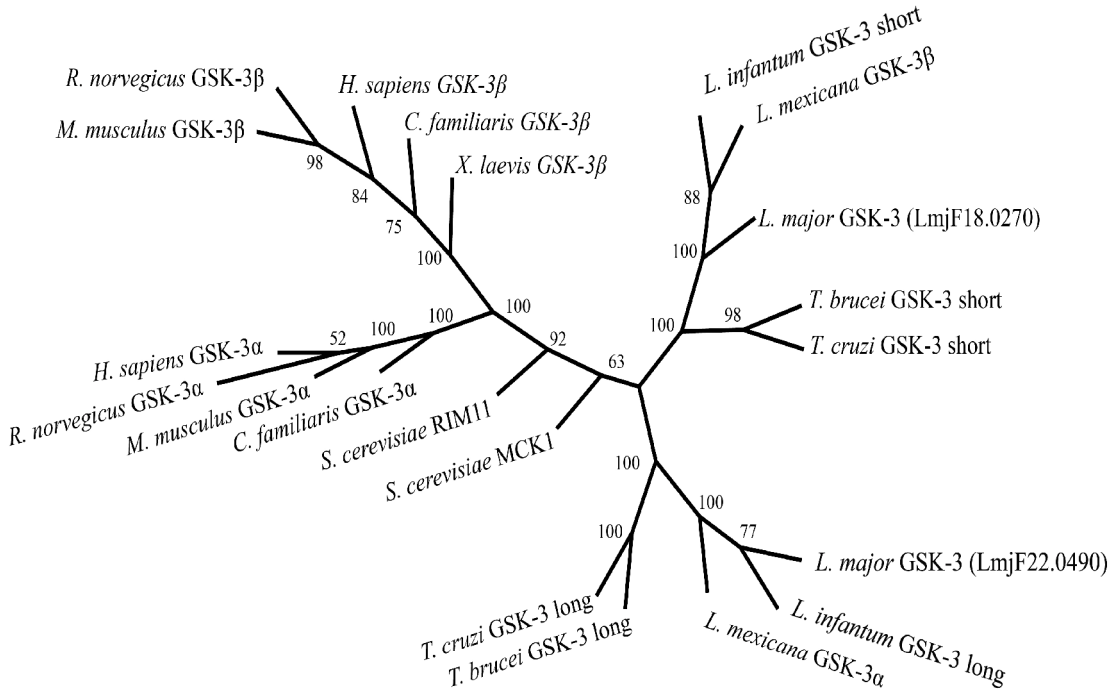

Using pairwise global alignments the resulting identity/similarity matrix (Table 2 of the revised manuscript) shows a higher identity (%) of the Leishmania GSK-3 short than

the GSK-3 long form to both the human GSK-3 forms although GSK-3s has a slightly higher identity to GSK-3β than to GSK-3α (Table 2).This does not allow us to unambiguously determine whether GSK-3s is equivalent to the GSK-3β mammalian form. Therefore we have renamed the studied homologue from GSK-3β to GSK-3 short.
Please refer to the Introduction and Results sections (lines 107-108 and lines 340-345 respectively). The annotation in the database has also been modified accordingly (Ac number EF620873).

Also, we have cited the suggested relevant publication (line 340).

2. Km values. Line 327-330 : < Km values for ATP and substrate for each kinase were measured; In order to determine IC50 values, we used ATP and substrates concentrations at the calculated Km values". Two questions/comments: (1) the enzymological raw data (e.g. Lineweaver-Burke plots) should be made available (e.g. as Supplementary Information). (2) From the statement above, it follows that both kinases have the same Km for ATP. Is that correct? That would be quite a coincidence!

As suggested by the reviewer Lineweaver-Burke plots are included in the revised manuscript as supplementary information (figure 3).

The Km values for ATP for both kinases are around 15 μM, specifically LdGSK3s and CRK3 Km for ATP was 15.2 μM and 14.78 μM respectively. So, we used 15 μM for the kinase assays, in order to be able to compare the IC50 values with the inhibitors.
We refer to this in the Materials and Methods section 2.12. (lines 282-285).

3. Effect of the inhibitors on amastigotes. Line 381 ff. If I understand the assay correctly, the infected macrophages are treated for 72h with the inhibitor, lysed, and the viability of parasites is measured 48 hours after lysis. If this is indeed the case, then the amastigotes are under drastically non-physiological conditions for 48 hours prior to measurement of viability. Can it be excluded that the function assigned to GSK3 in intracellular survival is in fact a function in stress response (i.e. parasites require GSK3 activity to survive stress caused by the sudden change to axenic conditions?). In other systems, GSK3 homologues are known to be involved in stress response (see for example Richard O, Paquet N, Haudecoeur E, Charrier B. "Organization and expression of the GSK3/shaggy kinase gene family in the moss Physcomitrella patens suggest early gene multiplication in land plants and an ancestral response to osmotic stress", J Mol Evol. 2005 Jul;61(1):99-113. Koh S, Lee SC, Kim MK, Koh JH, Lee S, An G, Choe S, Kim SR.T-DNA tagged knockout mutation of rice OsGSK1, an orthologue of Arabidopsis BIN2, with enhanced tolerance to various abiotic stresses. Plant Mol Biol. 2007Nov;65(4):453-66.) This would deserve a comment in the Discussion.

The reviewer's comment is correct. It could be speculated that in the intracellular amastigotes the function of LdGSK-3 may be linked among others to their response and adaptation to stress (acidic pH and shift in temperature). This is mentioned in the Discussion lines 653-655.

4. Figure 3. the text and legend to Fig. 3 do not provide sufficient information:
-There is no information on quality of the purified enzyme, other than the sentence (line 460) "we have purified LdGSK3 and CRK3 from L. donovani over-expressing transfectants and transgenic Lm promastigotes, respectively". One would really like to see a gel of the purified proteins, to be able to evaluate purity, especially considering the fact that the authors propose specific activity measurements (lines 465-466). To know how much kinase was used, one has to go to the Material & Methods section; even so, it is not clear what the source of enzyme is, as production from both bacteria and transgenic parasites is described. Please clarify.
-There is no mention of the concentration of 5-Me-6-BIO used in lane 3.
-Also, which casein was used (alpha, beta?)
-Finally, in Fig 3 the negative control is a heat-denatured extract; the kinase-dead enzyme would be a much better and more specific control. It is said (line 573) that "LdGSK-3<beta>/K49R, which was a kinase-dead mutant as confirmed by kinase assays".. why not include this in Fig. 3?

The requested information and relevant clarifications have been incorporated in the revised version.
- In particular we clearly mention that the LdGSK3s enzyme used for the kinase assays in Fig. 2 was purified from L. donovani LdGSK3s over-expressing transfectants (1 µg LdGSK-3s/reaction) (section 3.4, lines 417-418). We also mention this in the legend to Fig.2.
- A gel of the purified LdGSK3s and CRK3 is provided as supplementary figure 2 as suggested.
- In the material and methods section 2.12 (lines 273-274 and 290-291), we report that the source of the enzyme in both cases was from transgenic parasites.
-The concentration of 5-Me-6-BIO used in lane 3 was 4 µM, in order to achieve maximum inhibition of the enzyme (section 3.4, line 424). We also mention this in the legend to Fig.2.
- Concerning the type of casein we used it was dephosphorylated from bovine milk and was obtained from Sigma (C4032). It is usually used as a substrate for protein kinase assays (section 2.12, line 293).
-The reviewer's comment was correct. So, we have repeated the experiment and used the kinase-dead mutant LdGSK-3s/K49R as a negative control (new Fig. 2, lane 4)

5. Effect of over-expression of a kinase-dead mutant. One would expect that this would lead to a dominant-negative effect. In Fig. 7, there is no panel showing the sat-LdGSK3betaK49R in the absence of any inhibitor (the "control" line show presumably

wild-type parasites?). It would be interesting to see if overexpression of the mutant itself causes some phenotype.

The expression of the kinase-dead mutant did not lead to an apparent phenotype, as the cells still express the native kinase (Fig 5A). In Fig 6 (previously Fig 7) we do not show the sat-LdGSK-3s/K49R in the absence of any inhibitor, as they have the same phenotype with sat and sat-LdGSK-3s promastigotes. No apparent changes in parasite growth, cell cycle progression or morphology were observed. Fig. 5C shows that the cell cycle of the parasites expressing LdGSK-3s/K49R in the absence of the inhibitor is normal. We mention this in lines 552-553. In Fig. 6 control cells *(sat, sat-LdGSK-3s or sat-LdGSK-3s/K49R)* ***treated with 0.02% DMSO had a normal morphology. We mention this in lines 552-554.***

6. Structural modelling. The identification of the gatekeeper as a potential cause for difference in IC50s is interesting. One suggestion: since the authors rightly point out (line 683) in the context of GSK3 that apo structures are not as suitable as holo structures for docking experiments, it is important that that state that the structure (1E9H) they used in the context of CRK3 modelling is not just that of "CDK2" as they mention, but that of the CDK2-cyclinA complex, and hence much closer to an active configuration; it would be best to cite the original paper (Davies et al., Structure, 2001).

We have cited the original paper (Davies et al., Structure, 2001), concerning the CDK2-cyclinA complex, which was used to build the CRK3 homology model as suggested.

Minor and editorial points:

Several sentences are misconstructed and should be rewritten. Examples:
Line 416: "GSK-3<beta> homologues are almost identical in different Leishmania species and is the most well-studied mammalian isoform including crystallographical data."
Line 347 was rewritten: "GSK-3s homologues are almost identical in different Leishmania species and b) GSK-3s is slightly closer to the mammalian GSK-3<beta, the most well-studied isoform.

Line 467: "After determining the Km values for ATP and the respective for the substrates,."
Line 398 was rewritten: "After determining the Km values of both kinases for ATP and their respective substrates."

Line 672: "Moreover indirubin analogs, while potently inhibit leishmanial GSK-3<beta> (6BIO IC50=0.150<mu>M), they are not as efficient as in the case of the human homolog (6-BIO IC50=0.005<mu>M)."
Line 578 was rewritten: "While indirubin analogs potently inhibit leishmanial GSK-3s

(5-Me-6-BIO IC_{50}=0.09μM, 6BIO IC_{50}=0.150μM), they are not as efficient as in the case of the human homolog (5-Me-6-BIO IC_{50}=0.006μM, 6-BIO IC_{50}=0.005μM) (Meijer et al., 2003; Polychronopoulos et al., 2004).

Please give references for the TDZD-8 and SNS-032 inhibitors (line 494)
We give the references for all the inhibitors that we used in the kinase assays in the supplementary material under the name "Structurally divergent inhibitors".

For the benefit of the non-specialist reader, explain what a hypodiploid Leishmania cell is.
We have explained in the text that a hypodiploid Leishmania cell is a cell with <2N DNA content (line 447).

For reviewing purposes

"5-Me-6-BIO targeting the leishmanial GSK-3 short form affects cell-cycle progression and induces apoptosis-like death: exploitation of GSK-3 for treating leishmaniasis"

Evangelia Xingi [a], Despina Smirlis [a], Vassilios Myrianthopoulos [b], Prokopios Magiatis [b], Karen M. Grant [c], Laurent Meijer [d], Emmanuel Mikros [b], Alexios-Leandros Skaltsounis [b] and Ketty Soteriadou [a]

[a] Laboratory of Molecular Parasitology, Department of Microbiology, Hellenic Pasteur Institute, 127 Vas. Sofias Ave., 11521 Athens, Greece; [b] Laboratories of Pharmacognosy and Pharmaceutical Chemistry, Department of Pharmacy, University of Athens, Panepistimiopolis-Zografou, Athens 15771, Greece; [c] School of Health and Medicine, Lancaster University, LA1 4YB; [d] C.N.R.S., Cell Cycle Group, Station Biologique, B.P. 74, 29682 Roscoff cedex, Bretagne, France

Address correspondence to: Ketty P. Soteriadou, Laboratory of Molecular Parasitology, Department of Microbiology, Hellenic Pasteur Institute, 127 Vas. Sofias Avenue, 115 21 Athens, Greece, Tel.: +30 2106478841 Fax: +30 2106423498; e-mail address: ksoteriadou@pasteur.gr

Supplementary data associated with this article.

Abstract:

Indirubins known to target mammalian cyclin-dependent kinases (CDKs) and glycogen synthase kinase (GSK-3) were tested for their antileishmanial activity. 6-Br-indirubin-3'-oxime (6-BIO), 6-Br-indirubin-3'acetoxime and 6-Br-5methylindirubin-3'oxime (5-Me-6-BIO) were the most potent inhibitors of *L. donovani* promastigote and amastigote growth (IC_{50} values $\leq$ 1.2 μM). Since the 6-Br substitution on the indirubin backbone greatly enhances the selectivity for mammalian GSK-3 over CDKs, we identified the leishmanial GSK-3 homologues, a short (*Ld*GSK-3s) and a long one, focusing on *Ld*GSK-3s which is closer to human GSK-3β for further studies. Kinase assays showed that 5-Me-6-BIO inhibited *Ld*GSK-3s more potently than CRK3 (the CDK1 homologue in *Leishmania*), while 6-BIO was more selective for CRK3. Promastigotes treated with 5-Me-6-BIO accumulated in the S and G2/M cell-cycle phases and underwent apoptosis-like death. Interestingly, these phenotypes were completely reversed in parasites over-expressing *Ld*GSK-3s. This finding strongly supports that *Ld*GSK-3s is a) the intracellular target of 5-Me-6-BIO and b) involved in cell-cycle control and in pathways leading to apoptosis-like death. 6-BIO treatment induced a G2/M arrest, consistent with inhibition of CRK3, and apoptosis-like death. These effects were partially reversed in parasites over-expressing *Ld*GSK-3s suggesting that *in vivo* 6-BIO may also target *Ld*GSK-3s. Molecular docking of 5-Me-6-BIO in CRK3 and 6-BIO in human GSK-3β and *Ld*GSK-3s active sites predict the existence of functional/structural differences that are sufficient to explain the observed difference in their affinity. In conclusion, *Ld*GSK-3s is validated as a potential drug target in *Leishmania* and could be exploited for the development of selective indirubin-based leishmanicidals.

Keywords: *L. donovani* glycogen synthase kinase-3 short; 5-Me-6-BIO; 6-BIO; indirubins; apoptosis-like death; drug target

1. Introduction

Leishmaniasis is an umbrella term for a group of protozoan vector-borne parasitic diseases and manifests with three major forms, visceral, cutaneous and mucocutaneous. It is a significant cause of morbidity and mortality in developing countries, and affects about 2 million people per year mostly in tropical and subtropical regions (Alvar et al., 2006). Leishmaniasis is also an important public health and veterinary concern in Mediterranean countries (Dujardin, 2006). Chemotherapy for leishmaniasis is generally ineffective mainly due to the emerging drug-resistance and severe toxic side effects (Croft et al., 2006). Antimonials are used as first-line treatment despite their toxicity. In case of antimonial resistance, liposomal formulations of amphotericin B, not devoid of adverse side effects, are used (Croft et al., 2006). Miltefosine, the first oral drug, has proved to be highly effective against visceral leishmaniasis. However, miltefosine-resistant parasites have been obtained *in vitro* indicating that there is a risk of resistance emerging in the field. Consequently there is an urgent need to discover new targeted drugs against leishmaniases (Croft et al., 2006).

Leishmania species are transmitted to mammals by the bite of a sand fly vector. During a sandfly blood meal, *Leishmania* promastigotes pass into the mammalian host where they penetrate macrophages and, within their phagolysosomes, transform into the non-flagellated, non-motile amastigote form and multiply (Chang, 1983). These trypanosomatid protozoan parasites have developed unusual and unique features in their cell biology to ensure adaptation to the contrasting environments of their insect and mammalian hosts that are reflected in the complexity of their cell-cycle control and during their differentiation. Therefore, differences between cell-cycle control in *Leishmania* and mammals may lead to the identification of essential molecules regulating the parasite cell-cycle that could be exploited for rational drug design (Naula et al., 2005). Potential parasite candidate targets include cyclin-dependent kinases (CDKs), glycogen synthase kinases (GSK-3), Aurora kinases and mitogen activated protein kinases (MAPKs) (Naula et al., 2005). Recently, it was shown that *T. brucei* GSK-3 “short” is a potential drug target for trypanosomiasis therapy (Ojo et al., 2008). Efforts are therefore focused on the exploitation of kinase inhibitor

80 libraries for the identification and further development of inhibitors that selectively target parasite
81 kinases without damaging the host.

82 Indirubin analogues (collectively referred to as indirubins), a family of bis-indoles known for
83 over a century as a minor constituent of plant, animal and microorganism-derived indigo, are
84 powerful inhibitors of mammalian CDKs and GSK-3 by competing with ATP for binding to their
85 catalytic site (Meijer et al., 2003; Polychronopoulos et al., 2004). 6-bromo substituted indirubins
86 display higher selectivity for mammalian GSK-3 over CDKs (Meijer et al., 2003; Polychronopoulos
87 et al., 2004). In cell-based assays, indirubins display anti-mitotic and anti-tumoral activity and
88 induce arrest in G1 or G2/M phase of the cell-cycle, depending on the cell line (Hoessel et al., 1999;
89 Damiens et al., 2001). Specifically, 6-bromo-indirubin-3'-oxime (6-BIO) induces apoptotic death in
90 neuroblastoma cells (Ribas et al., 2006).

91 GSK-3 is a multifunctional serine/threonine kinase found in all eukaryotes. This enzyme is
92 known to play a key role in many cellular and physiological events, including Wnt signaling,
93 transcription, cell-cycle and differentiation, neuronal functions and circadian rhythm (Frame et al.,
94 2001; Doble and Woodgett, 2003). These functions of GSK-3 and its implication in many human
95 diseases such as Alzheimer's disease, non-insulin-dependent diabetes mellitus and cancer have
96 stimulated an active search for potent and selective GSK-3 inhibitors, like indirubins (Meijer et al.,
97 2004).

98 CRK3, a leishmanial CDK1 homologue, displaying 54% identity and 71% similarity with
99 human CDK1, has been validated as a drug target (Grant et al., 1998; Hassan et al., 2001). Three
100 indirubins (5-sulfonamide-indirubin-3'oxime, 5-SO_3Na-3'oxime and 5-SO_3H) have been shown to
101 inhibit CRK3 with IC_{50} values of 11 nM, 16 nM and 47 nM respectively and *L. donovani* infection
102 of mouse macrophages with IC_{50} values of 3.56 μM , 5.8 μM and 7.6 μM respectively (Grant et al.,
103 2004; Wells et al., 2006). *L. mexicana* promastigotes treated with indirubins displayed growth arrest
104 and disruption of cell-cycle, in line with the inhibition of a CDK (Grant et al., 2004).

In this study, sixteen indirubins were tested for their antileishmanial activity and three, 6-BIO, 6-BIA and 5-Me-6-BIO, were found to be the most powerful inhibitors of both *L. donovani* promastigotes and intracellular amastigotes growth. Since the 6-Br substitution on the indirubin backbone greatly enhances the selectivity for mammalian GSK-3 over CDKs, we identified the leishmanial GSK-3 homologues, a short (*Ld*GSK-3s) and a long one (*Ld*GSK-3l). We then investigated whether our compounds target *Ld*GSK-3s which is closer to human GSK-3β. *Ld*GSK-3s was identified as the predominant intracellular target of 5-Me-6-BIO. Evidence is also presented that *Ld*GSK-3s is involved in cell-cycle control as well as in pathways leading to apoptosis-like death.

2. Materials and methods

2.1. Cell culture

L. donovani (strain LG13, MHOM/ET/0000/HUSSEN) promastigotes and the murine macrophage J774 cell line (ATCC) were cultured in medium 199 (M199) and RPMI 1640 (RPMI) respectively, both supplemented with 10% heat inactivated fetal bovine serum (HI-FBS), 10 mM Hepes and antibiotics. Axenic *L. donovani* amastigotes were generated as previously described (Barak et al., 2005; Smirlis et al., 2006). Spleen-derived *L. donovani* amastigotes were maintained in Schneider's insect medium pH 5.5 supplemented with 20% HI-FBS at 37^0C. *L. donovani* transfectants with pLEXSY-sat, pLEXSY-sat-*Ld*GSK-3s, and pLEXSY-sat-*Ld*GSK-3s/K49R were cultured in M199 supplemented with 100 μg/ml nourseothricin (Jena Bioscience). *L. mexicana* CRK3his transfectants were cultured as described previously (Grant et al., 2004).

2.2. Chemical library

The library consists of sixteen indirubins (Table 1), synthesized as previously described, (Polychronopoulos et al., 2004; Ribas et al., 2006). The compounds were dissolved in DMSO at 10 mM and serial dilutions in DMSO were made (1 mM and 100 μM). Indirubins were diluted in culture medium to give the desired final concentrations.

2.3. Testing in vitro the antileishmanial activity of indirubins against L. donovani promastigotes, intracellular amastigotes and axenic amastigotes.

The Alamar blue assay (Mikus and Steverding, 2000) was applied for determining the antileishmanial activity of indirubins and Amphotericin B (Fungizone) was used as a reference drug. Stationary-phase *L. donovani* promastigotes (2×10^7 cells/ml) were seeded into 96-well flat bottom plates at a density of 2.5×10^6 cells/ml in 200 μl M199 without phenol red, containing increasing indirubin concentrations or the equivalent volume of the diluent DMSO, each in quadruplicate. The final concentration of DMSO was always <1% (v/v) and did not affect the growth of parasites. Following indirubin treatment for 72 h, Alamar blue (20 μl/well) was added and the plates were incubated at 26^0C for a further 12 h. Colorimetric readings were performed at a test wavelength of 550 nm and a reference wavelength of 620 nm. Comparison of DMSO-treated controls with samples allowed the calculation of the concentration of indirubin necessary to reduce the growth rate of promastigotes by 50% (IC_{50} values).

To evaluate the inhibitory activity of indirubins on intracellular amastigotes we treated infected macrophages for 72 h with indirubins and then assessed amastigote survival by lysing infected macrophages using the Alamar blue assay. Briefly, J774 macrophages (2×10^5 cells/ml in 200 μl RPMI) were left to adhere overnight at 37^0C in 5% CO_2 into 96-well flat bottom plates. Macrophages were infected with stationary-phase *L. donovani* promastigotes at a ratio of 10 parasites/macrophage and incubated for a further 24 h at 37^0C in 5% CO_2 as previously described (Papageorgiou and Soteriadou, 2002). Then the overlying medium was removed and cells were washed three times in fresh RPMI. Fresh RPMI was added containing increasing concentrations of

156 indirubins or the equivalent volume of the diluent DMSO, each in quadruplicate. After 72 h, the
157 medium was removed and infected cells were lysed by addition of 100 μl 0.01% SDS in PBS for 30
158 min at 37^0C. Then 100 μl Schneider's medium was added to each well, that contained the liberated
159 amastigotes (Papageorgiou and Soteriadou, 2002). Amastigote growth was assessed by the addition
160 of Alamar blue (20 μl/well) and the plates were incubated for 48 h at 37^0C. Comparison of DMSO-
161 treated controls with samples enabled the calculation of the degree to which infection had been
162 inhibited by the presence of indirubins and to calculate the concentration that reduces the number of
163 amastigotes by 50%.
164 *L. donovani* axenic amastigotes were treated with the inhibitors and the percentages of growth
165 inhibition were assessed by addition of Alamar blue after 72 h of treatment (Habtemariam, 2003).
166 In all cases, IC_{50} values were determined from dose-response curves via linear interpolation.
167
168 *2.4. Analysis of indirubin-treated promastigotes by flow cytometry (FACS).*
169 Stationary-phase (2×10^7 cells/ml) *L. donovani* promastigotes were seeded at 10^6 cells/ml in
170 M199 and incubated at 26^0C in the presence of DMSO (the diluent, used as control) or the tested
171 indirubin. Preparation of samples for FACS analysis of the cell-cycle was carried out as described
172 by Smirlis et al. (Smirlis et al., 2006). Exposed phosphatidylserine on the outer membrane of cells
173 and plasma membrane integrity of cells were assessed using Annexin V-FITC and PI staining
174 (Apoptosis Detection kit, R&D Systems). Preparation of samples for FACS analysis was performed
175 according to the manufacturer's instructions. In all cases, twenty thousand cells/sample were
176 analyzed, using a Becton Dickinson FACSCalibur flow cytometer and data were analyzed using the
177 Cell Quest software. All experiments were performed at least three times.
178
179 *2.5. Cellular and nuclear morphology.*
180 Stationary-phase *L. donovani* promastigotes were seeded at 10^6 cells/ml and incubated with
181 either 2 μM indirubin or DMSO for 24 and 48h. Cells were fixed in 2% paraformaldehyde, and

182 treated with 50 µg/ml RNaseA and 10 µg/ml propidium iodide (PI). Parasites were observed under a
183 TCSSP Leica Confocal fluorescence microscope. At least 100 cells from three independent
184 experiments were recorded for each condition.
185
186 *2.6. Cell count and viability assay*
187 Stationary-phase *L. donovani* promastigotes were seeded at 10^6 cells/ml and incubated with
188 either 2 µM 5-Me-6-BIO or DMSO for 24, 48h and 72 h. Cells were then washed twice in PBS,
189 resuspended in drug-free medium and allowed to recover for 24h, 48 h and 72 h. The viability assay
190 at different time points after exposure of parasites to 5-Me-6-BIO and drug removal was assessed
191 using 0.4% Trypan blue solution. Both total cell count and the percentages of viable and non viable
192 cells were recorded. The experiment was performed three times.
193
194 *2.7. In situ labeling of DNA fragments by TUNEL.*
195 *In situ* detection of DNA strand breaks was performed using the Cell Death Fluorescein
196 Detection kit (Roche Applied Science) following the manufacturer's instructions. Samples were
197 analyzed under a Zeiss fluorescence microscope at 120× magnification. The ratio of apoptosis
198 (apoptotic to total cells) was determined by counting at least 400 cells per group in three
199 independent experiments.
200
201 *2.8. Gene cloning and antibody production.*
202 The *L. donovani GSK-3s* gene was amplified by PCR from *L. donovani* (strain LG13,
203 MHOM/ET/0000/HUSSEN) genomic DNA, using a sense primer 5'-ACC GCC ATG GAC ATG
204 TCG CTC AAC GCT GC-3' and an antisense primer 5'-CCC CCT CGA GCT GCT TGC GAA
205 CTA GCT T-3', that were designed based on the gene coding for the shorter of the two *L. major*
206 *Friedlin* GSK-3 proteins (**LmjF18.0270**). The amplified PCR product was cloned into the *Nco*I-
207 *Xho*I site of pTriEx-1.1 vector (Novagen), a construct allowing the addition of a poly-Histidine

extention to the C-terminus of the recombinant protein (pTriEx-1.1-*Ld*GSK-3s). The cloned gene was then sequenced and compared with the short sequence of *L. infantum* GSK-3 (**LinJ18_V3.0270**). The *Ld*GSK-3s DNA and protein sequences were found to be identical to the *L. infantum* GSK-3s sequences. *Ld*GSK-3s nucleotide sequence was deposited in GenBank (**EF620873**). The pTriEx-1.1-*Ld*GSK-3s construct was transformed into bacteria and $(His)_6$–tagged *Ld*GSK-3 was purified by Metal-Affinity Chromatography (Qiagen Ni-NTA Superflow resin). *Ld*GSK-3s was detected using a polyclonal IgG His-probe antibody (1:500 dilution, stock solution 200 μg/ml, Santa Cruz Biotechnology) and a polyclonal anti-ratGSK-3β antibody. The recombinant protein was subsequently used to immunize a New Zealand white rabbit using the scheme described in a previous study (Smirlis et al., 2006). Affinity purified anti-*Ld*GSK-3s antibody was isolated by low pH elution of antibodies bound to purified *Ld*GSK-3s on nitrocellulose strips, as previously described (Smirlis et al., 2006).

2.9. Generation of transgenic promastigotes and purification of LdGSK-3s and CRK3.

The DNA encoding $(His)_6$–tagged *Ld*GSK-3s was amplified by PCR from the construct pTriEx-1.1-*Ld*GSK-3s, described above. Sense and antisense primers for the amplification were 5'-ACC GCC ATG GAC ATG TCG CTC AAC GCT GC-3' and 5' GCA GGC GGC CGC TGA GGT TAA TCA CTT AGT G 3' respectively. The PCR product was then cloned in the *NcoI* and *NotI* sites of the *Leishmania* expression vector pLEXSY-sat (pF4X1.4sat) (Jena Bioscience) to generate the pLEXSY-sat-*Ld*GSK-3s plasmid. The cloned gene was sequenced to confirm the correct orientation. Site-directed mutagenesis was performed on *Ld*GSK-3s in pLEXSY-sat-*Ld*GSK-3s construct, using the Phusion® Site-Directed Mutagenesis Kit (Finnzymes) following the manufacturer's protocol. Primers used for Lysine 49 to Arginine mutation (K49R) were as follows: Forward 5'-GAGCGTGGCGATCCGGAAGGTTATCCAGGAC-3' and Reverse 5'-ATGCCCGTCGACTTCTCCTTGCCTAGTTGCA-3'. The K49R mutation in the construct pLEXSY-sat-*Ld*GSK-3s/K49R was confirmed by sequencing.

L. donovani transfectants with pLEXSY-sat, pLEXSY-sat-*Ld*GSK-3s and pLEXSY-sat-*Ld*GSK-3s/K49R plasmids (supercoiled, transfected as episomes) were generated as previously described (Smirlis et al., 2006). Selection of transgenic promastigotes was performed in M199 containing 100 μg/ml nourseothricin.

Purification of *Ld*GSK-3s from *L. donovani* sat-*Ld*GSK-3s transfectants and of *Ld*GSK-3s/K49R from sat-*Ld*GSK-3s/K49R transfectants as well as of CRK3 from transgenic *L. mexicana* promastigotes was carried out as previously described (Grant et al., 2004). *Ld*GSK-3s and CRK3 were stored with 10% glycerol at -80^{0}C for kinase assays.

2.10. Immunoblotting

Parasites were suspended in lysis buffer (50 mM MOPs pH 7.5, 100 mM NaCl, 1 mM EDTA, 1 mM EGTA, 1 mM Na_3VO_4, 10 mM NaF, 1% Triton X-100) supplemented with protease inhibitors (0.1mg/ml leupeptin, 1 mM PMSF, 5 μg/ml aprotinin, 5 μg/ml pepstatin A, 1 mM phenanthroline) and Laemmli sample buffer was added. Whole cell lysates were resolved by 12% SDS-PAGE, transferred to nitrocellulose membranes and subsequently probed with the appropriate primary antibodies: a polyclonal anti-ratGSK-3β antibody [directed against the C-terminal sequence CAHSFFDELRDPNVK, residues identical between rat and *Ld*GSK-3s are underlined] (1:100 dilution, stock solution 500 μg/ml, Abcam); the generated anti-*Ld*GSK-3s rabbit polyclonal antibody (1:1000 dilution) and the polyclonal IgG His-probe antibody (1:200 dilution). After incubation with peroxidase-conjugated secondary antibody, 3,3′-Diaminobenzidine was used for detection.

To demonstrate equal loading of cells, the blot was stripped and re-probed with antiserum against *L. infantum* myo-inositol-1-phosphate synthase (LinJ14_V3.1450, INO1), reported to be equally expressed in *L. mexicana* promastigotes and amastigotes (Ilg, 2002). The *INO1* gene was PCR-amplified from *L. infantum* genomic DNA, using a sense primer 5'-CAAGGGATCCGATGACGCGTGACATGGACG-3' and an antisense primer 5'-GGCACTC

GAGCAGCATGTTGCTGTCGG-3', cloned into the *BamHI* and *XhoI* site of pTriEx-1.1, in frame with a C terminal his-tag, expressed in *E. coli* and purified on Ni-NTA resin. Anti-*Lin* INO1 antibody was produced and purified, using nitrocellulose strips with purified INO1, as previously described (Smirlis et al., 2006).

2.11. Immunofluorescence

Parasites were fixed in 2% formaldehyde and 0.05% glutaraldehyde. Cells were blocked in 50 mM NH_4Cl containing 3% BSA in PBS and treated with 50 μg/ml RNaseA. Nuclei were stained with 10 μg/ml PI followed by incubation for 5 h with either anti-*Ld*GSK-3s or the anti-ratGSK-3β antibodies (10 μg/ml or 5 μg/ml respectively) in PBS containing 0.1% Triton X-100 and 3% BSA. The bound antibody was detected with 1:100 diluted FITC conjugated anti-rabbit or anti-rat IgG antibody (Sigma). Cells were observed with a TCSSP Leica Confocal fluorescence microscope.

2.12. Kinase assays

Kinase assays were performed with purified *Ld*GSK-3s and CRK3 from *L. donovani* over-expressing transfectants and transgenic *L. mexicana* promastigotes respectively (supplementary Fig. 2). The kinase activity of *Ld*GSK-3s was assayed using GS-1 peptide (YRRAAVPPSPSLSRHSSPHQSpEDEEE) as a substrate; GS-1 peptide was patterned after the GSK-3 phosphorylation sites of mammalian glycogen synthase (Meijer et al., 2004). CRK3 kinase assays were performed using histone H1 substrate as previously described (Grant et al., 2004). All assays were performed in the kinase assay buffer (50 mM MOPS pH 7.2, 20 mM $MgCl_2$, 10 mM EGTA, 2 mM DTT) in the presence of [γ-^{33}] ATP (3,000 Ci/mmol; 1 mCi/ml) in a final volume of 30 μl and incubated for 30 min at 30^0C as previously described (Meijer et al., 2004). Initially the Km values for ATP and substrate for each kinase were measured. The Km values for ATP for both kinases were around 15 μM (15.2 μM for *Ld*GSK3s and 14.78 μM for CRK3). In order to determine the IC_{50} values with the inhibitors, we used ATP and substrate concentrations at the

286 calculated Km values. For both *Ld*GSK-3s and CRK3 15 μM ATP were used in the assays, in the
287 presence of 8.3 μM GS-1 peptide and 5 μM histone H1 respectively. Ki values for each inhibitor
288 were calculated using the Cheng-Pursoff equation [Ki= IC_{50}/ (1+ S/Km)]. Kinase assays were also
289 performed using the Kinase Luminescent Assay Kit (Promega), following the manufacturer's
290 instructions, and gave comparable results.

291 *Ld*GSK-3s activity (purified from *L. donovani* over-expressing transfectants, 1 μg
292 enzyme/reaction) was also determined using potential protein substrates: *L. infantum* histone H1
293 (LeishH1), mammalian histone H1 (Sigma), axin (recombinant, purified from bacteria), myelin
294 basic protein and casein (dephosphorylated from bovine milk, Sigma), (approximately 1 μg
295 substrate/reaction). LeishH1 was expressed in bacteria as a fusion protein with Glutathione-S-
296 Transferase (GST) and purified with Sepharose 4B-Glutathione beads as previously described
297 (Smirlis et al., 2006). LeishH1 recombinant protein was cleaved from the GST moiety by thrombin
298 treatment (Smirlis et al., 2006). *In vitro* phosphorylation of protein substrates was performed in the
299 kinase assay buffer. After 30-min incubation at 30^0C, in the presence of [γ-^{32}P] ATP (6,000
300 Ci/mmol, 10 mCi/ml) in a final volume of 30 μl, the kinase reaction was stopped by addition of
301 Laemmli buffer (Meijer et al., 2004). The protein substrates were resolved by 12% SDS-PAGE,
302 stained with Coomassie blue and their phosphorylation level was visualized by autoradiography.
303

304 *2.13. Homology modeling*

305 The homology model of parasite GSK-3s was based on the crystal structure of the human
306 GSK-3β complexed with 6-BIO (pdb 1Q41) and the respective of CRK3 on the template structure
307 of human CDK2-cyclin A (pdb 1E9H), (Davies et al., 2001). Model building was performed with
308 MODELLER v. 6 program (Sali and Blundell, 1993) and stereochemical validation with
309 PROCHECK program (Laskowski, 1991). Docking was performed with a Monte Carlo search
310 algorithm. Ligand partial charges were calculated in a semi-empirical level by MOPAC6 (AM1
311 hamiltonian) (Stewart, 1990).

3. Results

3.1. Evaluation of the antileishmanial effect of indirubins towards L. donovani promastigotes and amastigotes.

The Alamar blue assay (Mikus and Steverding, 2000) in a 96-well format, was used for the primary screening and subsequent monitoring of the growth of *L. donovani* promastigotes and axenic amastigotes exposed to indirubins. The same assay was adapted and used for estimating the growth of intracellular amastigotes 48 h after lysis of the infected macrophages treated for 72 h with the indirubins. In the initial screening, sixteen indirubins were tested at 10 μM. Nine of the compounds did not significantly affect parasite growth even when used at a higher concentration of 50 μM. Four out of the sixteen compounds tested significantly inhibited *Leishmania* growth and their IC_{50} values were determined, (Table 1). More specifically, 6-BIO, 6-BIA and 5-Me-6-BIO inhibited promastigote growth with an IC_{50} of 0.8±0.1 μM, 0.9±0.1 μM and 1.2±0.2 μM respectively (Table 1). 5-BIO inhibited promastigote growth with an IC_{50} of 5.2±1.6 μM (Table 1). Interestingly, 6-BIO, 6-BIA, 5-Me-6-BIO and 5-BIO were also found to significantly inhibit the growth of both *L. donovani* intracellular and axenic amastigotes with IC_{50} values ranging from 0.75±0.05 μM to 1±0.2 μM respectively (Table 1). N1-methyl derivatives of 6-BIO and 6-BIA did not inhibit the growth of either promastigotes or amastigotes, consistent with the inactivation of indirubins as kinase inhibitors by this modification (Meijer et al., 2003).

All four compounds did not affect the growth of macrophages at the concentration used, but as determined using the same assay, they were toxic for host cells at significantly higher concentrations (IC_{50} values >25 μM). Amphotericin B used as a reference drug inhibited promastigote and amastigote (intracellular or axenic) growth with IC_{50} values of 0.1±0.01 μM and 0.2±0.02 μM respectively.

338 *3.2. Molecular characterization of LdGSK-3s: expression and localization in L. donovani life cycle.*

339 Since 6-bromo indirubins are powerful and selective inhibitors of mammalian GSK-3 (Meijer et
340 al., 2003; Polychronopoulos et al., 2004) we searched in the *Leishmania GeneDB* database for
341 GSK-3 homologues (Parsons et al., 2005). Two GSK-3 encoding genes were found in the
342 *Leishmania* genome by BLAST homology searches, a short and a long version. Comparison of the
343 amino acid identities of the two human GSK-3 orthologues versus the two *L. infantum* forms
344 revealed that GSK-3s is closer than GSK-3l to human GSK-3α and GSK-3β. However, GSK-3s has
345 a slightly higher identity to GSK-3β than to GSK-3α (Table 2). This does not allow us to
346 unambiguously determine whether GSK-3s is equivalent to the GSK-3β mammalian form.

347 We focused on the GSK-3s isoform for further studies, since: a) the GSK-3s homologues are
348 almost identical in different *Leishmania* species and b) GSK-3s is slightly closer to the mammalian
349 GSK-3β, the most well-studied isoform. The *GSK-3s* gene in *L. infantum*, in *L. major* and in *L.*
350 *mexicana* is located on chromosome 18 and encodes a protein of 355 amino acids with a predicted
351 molecular mass of 40.7 kDa. BLASTP analysis showed that the identified *L. donovani GSK-3s*
352 gene was identical to the *L. infantum GSK-3* short gene and almost identical to *L. major and L.*
353 *mexicana GSK-3* short *and GSK-3β* genes respectively (98% identity and 99% similarity),
354 (supplementary Fig. 1). *Ld*GSK-3s shares 49% sequence identity and 68% similarity with hGSK-
355 3β. It also shares 65% identity and 80% similarity with *T. brucei* GSK-3 "short", 47% identity and
356 67% similarity with *Danio rerio* GSK-3β, 42% identity and 64% similarity with *Plasmodium*
357 *falciparum* GSK-3, and 49% identity and 68% similarity with *Mus musculus* GSK-3β
358 (supplementary Fig. 1).

359 *Ld*GSK-3s was detected in *L. donovani* extracts using an affinity-purified anti-*Ld*GSK-3s
360 polyclonal antibody (raised against the recombinant protein expressed in *E.coli*) and a commercially
361 available polyclonal anti-ratGSK-3β antibody (raised against the C-terminal sequence of rat GSK-
362 3β). The ~40 kDa protein detected by both antibodies is in line with the predicted molecular mass of
363 *Ld*GSK-3s. Western blot analysis indicated that the level of expression of *Ld*GSK-3s in *L. donovani*

364 stationary and logarithmic-phase promastigotes (10^7 cells/lane) was comparable (Fig. 1A, lanes S
365 and L respectively). *Ld*GSK-3s was also detected in spleen-derived *L. donovani* amastigotes and
366 axenic amastigotes (10^7 cells/lane), (Fig. 1A, lanes Am and Ax respectively). Scanning
367 densitometry of the detected bands revealed that *Ld*GSK-3s expression level was about 3-fold lower
368 in amastigotes. As a control for loading equal number of cells, the blot was stripped and re-probed
369 with the antiserum against *L. infantum* myo-inositol-1-phosphate synthase (*Lin*INO1), a 46 kDa
370 protein whose level of expression is constitutive during promastigote growth and which is equally
371 expressed in promastigotes and amastigotes, (Ilg, 2002; Rosenzweig et al., 2008) (Fig. 1B). No
372 protein band was detected when pre-immune serum was used, as a negative control, (Fig. 2C, lane
373 S, Ax). *Ld*GSK-3s was also recognized by the anti-ratGSK-3β antibody (Fig. 2D lane S). Similarly,
374 the mouse GSK-3β (a 47 kDa protein) in J774 cell extracts (9×10^5 cells/lane) was detected using
375 both antibodies (Fig. 1A and D, lane J774). This result shows the cross reactivity of the two
376 antibodies with mammalian and leishmanial GSK-3s.

377 The intracellular localization of *Ld*GSK-3s in *L. donovani* promastigotes and axenic amastigotes
378 was detected by immunofluorescence using both the affinity-purified anti-*Ld*GSK-3s and the anti-
379 ratGSK-3β antibodies. Immunostaining of *L. donovani* logarithmic-phase promastigotes showed
380 that *Ld*GSK-3s is localized in the parasite cytoplasm and flagellum (Fig. 1E). FITC-staining in the
381 parasite nucleus or kinetoplast was detected at background levels. Interestingly, *Ld*GSK-3s was
382 localized mainly in the parasite nucleus and flagella in stationary-phase promastigotes (Fig. 1E).
383 *Ld*GSK-3s was also detected in logarithmic-phase axenic amastigotes but the pattern of
384 immunostaining was different from both logarithmic- and stationary-phase promastigotes: more
385 condensed and localized immunostaining in the cytoplasm of axenic amastigotes (Fig. 1E). In all
386 cases staining with the two antibodies was similar and therefore only that with the affinity-purified
387 anti-*Ld*GSK-3s is shown.

388

389 *3.3. LdGSK-3 s and CRK3 inhibitor screen.*

Since 6-bromo indirubins are powerful inhibitors of mammalian CDKs and GSK-3 (Meijer et al., 2003; Polychronopoulos et al., 2004) we thought to examine whether they also target *Ld*GSK-3s and/or CRK3. To this end we have purified *Ld*GSK-3s and CRK3 from *L. donovani* over-expressing transfectants and transgenic *L. mexicana* promastigotes respectively (supplementary Fig. 2) and their kinase activities were assayed using GS-1 peptide and histone H1 as substrates respectively, in the presence of the indirubins that displayed maximum growth inhibition in the cell-based assay. Of note is that *L. donovani* CRK3 displays 99% sequence identity with *L. mexicana* CRK3, which was used for the inhibitor screen. Specific activities of the enzymes were found to be 800 U/mg for *Ld*GSK-3s and 750 U/mg for CRK3. After determining the Km values of both kinases for ATP and their respective substrates, (supplementary Fig. 3), dose-response curves were used to calculate the IC_{50} values (Table 3). 6-BIO, 6-BIA, 5-BIO and 5-Me-6-BIO inhibited *Ld*GSK-3s with IC_{50} values of 0.15, 0.17, 0.35 and 0.09 μM respectively, whereas CRK3 was inhibited with IC_{50} values of 0.02, 0.25, 0.7 and 0.65 μM respectively (Table 3). Thus, 5-Me-6-BIO displayed an approximately 7-fold selectivity for *Ld*GSK-3s over CRK3, while 6-BIO was about 7-fold more active towards CRK3 than *Ld*GSK-3s. 6-BIA inhibited CRK3 ~1.5-fold more than *Ld*GSK-3s. N1-methyl derivatives of 6-BIO and 6-BIA, that displayed no growth inhibition in the cell-based assay, were inactive on both kinases (Table 3).

To compare the inhibitory activity of indirubins against *Ld*GSK-3s and CRK3, IC_{50} values were evaluated relatively to Ki values of the inhibitors which were equal to ½ of IC_{50} values because kinase assays were performed in ATP concentration equal to the Km for ATP. 5-Me-6-BIO inhibited *Ld*GSK-3s with a Ki of 0.045 μM and CRK3 with a Ki of 0.325 μM . 6-BIO inhibited *Ld*GSK-3s with a Ki of 0.075 μM and CRK3 with a Ki of 0.01 μM.

Indirubins 6-FIO, 6-ClIO and 6-IIO substituted at position 6 with the halogens F, Cl and I respectively were found less active towards both kinases (Table 3) as well as towards *L. donovani* promastigotes (IC_{50} values >3 μM). Interestingly, 6-iodo substituted indirubin was 5-fold more active towards *Ld*GSK-3s.

3.4. Substrate selectivity of LdGSK-3s.

Substrate selectivity of *Ld*GSK-3s purified from *L. donovani* over-expressing transfectants (1 μg *Ld*GSK-3s/reaction) was investigated using potential substrates: LeishH1, axin, myelin basic protein (MBP), mammalian histone H1 and casein (Fig. 2). LeishH1 was chosen because it possesses the consensus recognition motif for phosphorylation by GSK-3β: S/TXXXS/T(P), where X is any amino-acid (Doble and Woodgett, 2003). *Ld*GSK-3s shows no autophosphorylation when the kinase assay is performed without substrate (Fig. 2, lane 1). Phosphorylation of LeishH1 by *Ld*GSK-3s (Fig 2, lane 2) was inhibited when the kinase reaction was performed in the presence of 4 μM 5-Me-6-BIO, (Fig 2, lane 3). Control kinase reaction was also performed, using the kinase-dead mutant *Ld*GSK-3s/K49R with LeishH1 as a substrate (Fig 2, lane 4). The GST moiety was not phosphorylated by *Ld*GSK-3s (Fig 2, lane 5). Axin (~ 55 kDa), MBP (18.4 kDa), mammalian histone H1 (21.5 kDa) and casein (23 kDa) were found to be good protein substrates of *Ld*GSK-3s (Fig 2, lanes 6-9). The basic nature of histones and the rich content in prolines in casein that affects its conformation cause them to migrate slower in SDS-PAGE. None of the substrates tested displayed intrinsic phosphorylation (data not shown). However, more experimental data is needed to prove *in vivo* interaction of *Ld*GSK-3s and LeishH1, as the kinase phosphorylating LeishH1 has not been identified so far.

3.5. Cell-cycle disruption and induction of apoptosis-like death in 5-Me-6-BIO- and 6-BIO- treated L. donovani promastigotes.

The cell-cycle distribution of promastigotes incubated with 5-Me-6-BIO and 6-BIO was analyzed using flow cytometry (Fig. 3A). Promastigotes treated with 1 μM 5-Me-6-BIO for either 24 h or 48 h resulted in a decrease in the G0/G1 DNA content (40.9% and 37.5% respectively compared to 66% of control parasites) and an increase in cells in S phase (13.4% and 11% respectively compared to 7.3% of control cells) with a concomitant increase in the G2/M phase of

442 the cell-cycle (43.7% and 49.4% respectively compared to 23.9% of control cells). Treatment of
443 promastigotes with 6-BIO resulted in an increase in the proportion of cells with G2/M DNA
444 content, the latter being time and dose dependent. After 48 h of treatment with 2 μM 6-BIO 74.5%
445 of cells were in G2/M ((Fig 3B). Control cells treated with the diluent (0.01% or 0.02% DMSO)
446 had a normal cell-cycle distribution at all time-points studied (66% G0/G1, 7.66% S, 23.8% G2/M).
447 Of note is that cells treated with 2 μM 5-Me-6-BIO for 24 h and 48 h had a high percentage of
448 hypodiploid cells (<2N DNA content) and accumulated in the sub-G0 phase (29.8% and 40%
449 respectively) which is indicative of apoptotic-like cell death (Fig. 3A).

450 In order to investigate whether 5-Me-6-BIO- and 6-BIO- induced apoptotic-like mechanisms in
451 *Leishmania* we used double staining with Annexin V-FITC and PI. This staining allows the
452 differentiation between early apoptotic (Annexin V-FITC positive), late apoptotic (Annexin V-
453 FITC and PI positive), necrotic (PI positive) and viable cells (unstained). Incubation of cells with
454 0.02% DMSO showed negative staining for both Annexin V and PI, as 97.8% of cells were viable
455 at all time-points (Fig. 3C, control). In the positive control for necrosis, 39.23% of Triton X-100-
456 treated promastigotes were found to be PI positive (Fig. 3C, Triton X-100). 49.23% of cells treated
457 with 4 mM hydrogen peroxide (H_2O_2), used as a positive control for apoptosis, for 40 min (Das et
458 al., 2001) were found to be late apoptotic, 2.97% early apoptotic and 13.99% necrotic (Fig. 3C,
459 H_2O_2). Treatment of promastigotes with 2 μM 5-Me-6-BIO for 48 h resulted in a high percentage of
460 Annexin V positive cells (57.9%), of which 6.42% were early apoptotic and 51.48% were late
461 apoptotic, while viable cells were 38.42% (Fig. 3C, 5-Me-6-BIO). The percentage of cells
462 undergoing early apoptosis was higher than that of late apoptosis (29.35% versus 12.03%) when
463 cells were treated for 24 h whereas treatment of promastigotes with 2 μM 5-Me-6-BIO for 72 h
464 resulted in an increase in PI positive cells, as 26.04% of cells were necrotic and 61.2% late
465 apoptotic, while only 10.83% of cells were viable (data not shown). Treatment of promastigotes
466 with 2 μM 6-BIO for 48 h resulted in an increased labeling with Annexin V. Early and late

apoptotic cells together constituted about 40.4% of the cells: 20.18% of cells were late apoptotic and 20.23% were early apoptotic compared to controls (Fig. 3C, 6-BIO).

To further study whether the observed effect of indirubins was due to apoptosis-like death we monitored morphological and nuclear changes by confocal microscopy. Control cells displayed a normal elongated morphology with two discrete stained organelles, the nucleus and the kinetoplast (Fig. 4, control). Promastigotes exposed to 5-Me-6-BIO for 24 h showed rounded forms, cell shrinkage and variations in the length of their flagella as well as nuclear changes characteristic of apoptosis-like death; apoptotic nuclei were identified by their bright red fluorescence, which included a certain degree of condensation of nuclear chromatin in 36% of cells and breakdown of the nuclear material in 41% of cells (Fig. 4, 5-Me-6-BIO, 24 h). At the 48 h-time point, 78% of cells exhibited a totally fragmented nucleus (Fig. 4, 5-Me-6-BIO, 48 h). Formation of zoids was not observed (Grant et al., 2004). Treatment with 2 μM of 6-BIO for 24 h had less pronounced morphological alterations. It resulted in cells with either a normal morphology with a discrete kinetoplast and a nucleus (approximately 38% of cells) or in rounded-shaped with short flagella and condensed nuclear chromatin (~62%) (Fig. 4, 6-BIO, 24 h). After treatment with 6-BIO for 48 h, the majority of parasites (75%) displayed an aberrant morphology, with round body shape and short flagella of which 36% displayed nuclear condensation and 39% nuclear fragmentation (Fig. 4, 6-BIO, 48 h).

Since the cellular effects induced by 5-Me-6-BIO were more pronounced than those of 6-BIO we investigated whether they were reversibile after drug removal. To this end the recovery of cells following exposure to 5-Me-6-BIO for 24h, 48 h and 72 h was assessed 24h, 48 h and 72 h after the drug removal. Control cells treated with 0.02% DMSO were viable at all time-points tested (100% viability). As shown in Fig. 3D treatment of cells with 5-Me-6-BIO for 24 h followed by incubation with fresh medium up to 72 h resulted in full recovery of cells. After 48 h of treatment, about 48% of cells were viable. Further incubation in fresh medium for 24 h resulted in an increase in the percentage of viable cells (77.7%). At the 48 h and 72 h time-points, a full recovery of the cells was

observed. In contrast, incubation for 72 h with 5-Me-6-BIO resulted in about 89% dead cells. Removal of the drug resulted in irreversible cytotoxicity.

3.6. LdGSK-3s over-expression in L. donovani counteracts 5-Me-6-BIO- and 6-BIO- induced growth inhibition, cell-cycle progression and apoptosis-like death

To investigate whether *Ld*GSK-3s is the intracellular target of 5-Me-6-BIO and whether all the observed phenotypes in the presence of 5-Me-6-BIO could be attributed to inhibition of this kinase, we have generated transgenic *L. donovani* promastigotes over-expressing *Ld*GSK-3s and compared their susceptibility to 5-Me-6-BIO with that of control transfectants bearing the plasmid alone. We also investigated whether over-expression of *Ld*GSK-3s affected the growth inhibitory effect of 6-BIO. As a control, we generated transgenic promastigotes overexpressing *Ld*GSK-3s/K49R, which was a kinase-dead mutant as confirmed by kinase assays (Fig. 2, lane 4). The mutation of the catalytic residue Lys 49 to Arg was designed based on the homology model of *Ld*GSK-3s and on the widely used mutation of Lys 85 to Arg or Ala of mammalian GSK-3β, which results in a kinase-dead protein (He et al., 1995). Over-expression of *Ld*GSK-3s and expression of *Ld*GSK-3s/K49R in the *Ld*GSK-3s and *Ld*GSK-3s/K49R transfectants was confirmed by immunoblotting using both a His-probe antibody and the anti-*Ld*GSK-3s antibody (Fig. 5A). The *Lin*INO1 antibody was used as a loading control. Scanning densitometry showed that the level of expression of *Ld*GSK-3s in *Ld*GSK-3s and *Ld*GSK-3s/K49R transfectants was about 2-fold higher in comparison with sat transfectants (Fig. 5A). Expression of the kinase-dead mutant did not cause any apparent changes in parasite growth or morphology.

The susceptibility of stationary-phase *L. donovani* sat, sat-*Ld*GSK-3s and sat-*Ld*GSK-3s/K49R transfectants to increasing concentrations of 5-Me-6-BIO was assessed after 24h, 48 h and 72 h of treatment by cell counting. The IC_{50} of 5-Me-6-BIO after 24h, 48h and 72h of treatment of the sat-transfectants was 1.5±0.2 μM, 1.25±0.1 μM and 1.2±0.1 μM respectively, which are comparable with the IC_{50} against wild type promastigotes (Table 1), whereas its respective IC_{50} for the *Ld*GSK-

519 3s over-expressing transfectants was 3.6±0.3 μM, 3.2±0.2 μM and 2.8±0.2 μM (Fig. 5B). As
520 expected, the sat-*Ld*GSK-3s/K49R transfectants were inhibited by 5-Me-6-BIO with IC_{50} values of
521 1.7±0.1 μM after 24 h, 1.4±0.1 μM after 48 h and 1.3±0.05 μM after 72 h, which are comparable
522 with the respective IC_{50} values against sat-transfectants (Fig. 5B).

523 Treatment of the *Ld*GSK-3s over-expressing transfectants with 6-BIO resulted in a clear
524 decrease in their sensitivity, with IC_{50} values of 4.8±0.5 μM after 24 h, 2.2±0.4 μM after 48 h of
525 treatment and 1.57±0.3 μM after 72 h of treatment, which were approximately 2-fold higher
526 compared to IC_{50} values of sat and sat-*Ld*GSK-3s/K49R transfectants (Fig. 5D). Sat and sat-
527 *Ld*GSK-3s/K49R transfectants treated with different 6-BIO concentrations displayed growth
528 inhibition with approximately the same IC_{50} values as *L. donovani* wild type promastigotes. Sat
529 transfectants were inhibited with IC_{50} values of 2.75±0.45 μM after 24 h of treatment, 1.3±0.3 μM
530 after 48 h of treatment and 0.78±0.25 μM after 72 h of treatment and sat-*Ld*GSK-3s/K49R
531 transfectants were inhibited with IC_{50} values of 2.9±0.3 μM after 24 h, 1.3±0.2 μM after 48 h and
532 0.85±0.2 μM after 72 h (Fig. 5D).

533 Flow cytometry analysis of the DNA content of control *L. donovani* sat, sat-*Ld*GSK-3s and sat-
534 *Ld*GSK-3s/K49R over-expressing transfectants, treated with 0.02% DMSO, showed that cells had a
535 normal cell-cycle distribution: 67.9% G1, 6.9% S, 23.2% G2 (Fig. 5C, control). Interestingly, sat-
536 *Ld*GSK-3s promastigotes incubated with 2 μM 5-Me-6-BIO for 48 h had a normal cell-cycle
537 distribution: 62% G1, 5.45% S and 30.5% G2 (Fig. 5C, 5-Me-6-BIO), whereas 40% of sat and sat-
538 *Ld*GSK-3s/K49R transfectants were hypodiploid and accumulated in the sub-G0 phase (Fig. 5C),
539 as was observed with wild type promastigotes (Fig. 3A).

540 However, as shown in Fig. 5C, *Ld*GSK-3s over-expressing promastigotes treated with 6-BIO
541 displayed a less pronounced increase in G2/M (41.7% compared to 74.5% in 6-BIO-treated wild
542 type parasites) and a less pronounced decrease in G0/G1 (46% compared to 15.8% in 6-BIO-treated
543 wild type parasites) (Fig. 5C, sat-*Ld*GSK-3s). In contrast, sat transfectants incubated with 2 μM 6-
544 BIO for 48 h were comparable with wild type promastigotes and arrested at G2/M (74.9%

545 compared to 23.2% of control), with a significant decrease in G0/G1 (19.3% compared to 67.9% of
546 control) (Fig. 5C, 6-BIO). Similar results with the latter were obtained for the sat-*Ld*GSK-3s/K49R
547 transfectants which had the following cell-cycle distribution: 21.8% G0/G1, 4.4% S and 71.7%
548 G2/M.

549 Since *Ld*GSK-3s over-expression resulted in a significantly reduced growth inhibition and a
550 normal cell-cycle distribution upon 5-Me-6-BIO-treatment, we investigated whether *Ld*GSK-3s
551 over-expression affected apoptosis-like death using the terminal deoxynucleotidyltransferase-
552 mediated dUTP nick end labeling (TUNEL) assay, which detects apoptosis at a single-cell level.
553 Control cells treated with 0.02% DMSO (sat, sat-*Ld*GSK-3s or sat-*Ld*GSK-3s/K49R) containing
554 intact genomic DNA were not stained, (Fig. 6, control). Promastigotes treated with 4 mM H_2O_2 for
555 6 h, served as a TUNEL positive control, as about 99% of cells showed positive nuclear staining
556 (Fig. 6, H_2O_2). Sat transfectants exposed to 2 μM 5-Me-6-BIO for 48 h were about 68% TUNEL
557 positive and their morphology was dramatically affected in comparison to the normal elongated
558 morphology of control cells (Fig. 6, sat/5-Me-6-BIO). Treated cells displayed an aberrant
559 morphology, with round body shape and cell shrinkage. Sat-*Ld*GSK-3s transfectants treated with 2
560 μM 5-Me-6-BIO for 48 h were not positive for TUNEL reactivity, only a background staining of
561 about 3% was detected and their morphology was not affected (Fig. 6, sat-*Ld*GSK-3s/5-Me-6-BIO).
562 Sat-*Ld*GSK-3s/K49R transfectants were about 70.4% TUNEL positive (Fig. 6, sat-*Ld*GSK-
563 3s/K49R/5-Me-6-BIO).

564 The contribution of *Ld*GSK-3s in the apoptosis-like death observed in 6-BIO treated
565 promastigotes was also studied using the over-expressor lines. Whereas sat transfectants exposed to
566 2 μM 6-BIO for 48 h were ~ 50% TUNEL positive and their morphology was dramatically affected,
567 *Ld*GSK-3s over-expressing transfectants were resistant to the effects of 6-BIO and displayed a
568 much milder phenotype. Only 20% of the cells were TUNEL positive and their morphology was not
569 significantly affected when compared to control cells (Fig. 6, sat/6-BIO and sat-*Ld*GSK-3s/6-BIO

570 respectively). As expected, sat-*Ld*GSK-3s/K49R transfectants were about 52.9% TUNEL positive
571 (Fig. 6, sat-*Ld*GSK-3s/K49R/6-BIO).
572
573 *3.7. Structure Activity Relationships studies of indirubin-leishmanial kinases interactions using*
574 *molecular simulations.*
575 Biological results imply that indirubins inhibit leishmanial kinases. Interestingly, the selectivity
576 observed for 6-substituted indirubins towards GSK-3 with respect to the CDKs in human is reversed
577 in the case of *Leishmania* and the homologous kinases (GSK-3 and CRK3) with the exception of
578 the 6-iodo as well as the bisubstituted 5-Me-6Br analogs. While indirubins potently inhibit the
579 leishmanial GSK-3s (5-Me-6-BIO with an IC_{50}=0.09μM and 6BIO with an IC_{50}=0.150μM), they
580 are not as efficient as in the case of the human homolog (5-Me-6-BIO with an IC_{50}=0.006μM and
581 6-BIO with an IC_{50}=0.005μM) (Meijer et al., 2003; Polychronopoulos et al., 2004).
582 Both pairs of homologous kinases are highly similar and the observed differences in affinity
583 could possibly be explained by the key residue differences of the binding cavity. In order to obtain
584 insight in the inhibitor-protein interactions, we built homology models of the parasite kinases
585 (supplementary data). Despite the fact that important residues of the leishmanial GSK-3s seem to be
586 well conserved (supplementary Fig. 1), there were two major differences between the two kinases
587 located in the binding pocket: a) the replacement of $Gln185^{hGSK\text{-}3\beta}$ by $His155^{LGSK\text{-}3s}$ in the sugar-
588 binding region and b) the replacement of the "gatekeeper" $Leu132^{hGSK\text{-}3\beta}$ by $Met100^{LGSK\text{-}3s}$. The
589 "gatekeeper" residue controls access to a hydrophobic cavity of the binding pocket and is
590 considered as a selectivity determinant of most ATP competitive kinase inhibitors (Bohmer et al.,
591 2003). In the majority of the members of the GSK-3 family (CMGC III), the gatekeeper is a leucine,
592 except for MCK-1 kinase which has a methionine (Hanks and Quinn, 1991). However, a
593 methionine is present in *Leishmania*, *Trypanosoma brucei* and *Plasmodium falciparum* GSK-3s,
594 (supplementary Fig. 1).

595 Docking calculations were performed in order to study the binding mode/interactions of
596 indirubins in the binding cavity of each kinase. In each case the inhibitor was anchored at the kinase
597 backbone through the formation of three hydrogen bonds in the usually observed adenine type of
598 interaction (Figure 7A), while the substituent of position 6 was positioned in the hydrophobic cavity
599 formed by the sidechain of the gatekeeper residue interacting with it. In human GSK-3β the leucine
600 gatekeeper can form only hydrophobic interactions with the 6 substituent of indirubin. However, in
601 the parasite kinase the mode of interactions accommodated by the methionine gatekeeper is more
602 complicated, resulting in a larger entropic and desolvation cost upon inhibitor binding
603 (supplementary data). Such a net effect for the replacement of the leucine gatekeeper to a
604 methionine could be considered as unfavorable for binding affinity, accounting for the loss of
605 binding affinity in a common trend for all indirubins tested, which is in consistency with IC_{50}
606 results obtained from kinase assays.
607 The higher affinity for CRK3 (reversal of selectivity with respect to the human kinases)
608 demonstrated by 6-substituted indirubins tested with the exception of 6-IIO, 5-Me-6-BIO and
609 partially of 6-BIA compared to the affinity for *Ld*GSK-3s could be explained by the formation of a
610 hydrogen bond between $Tyr101^{CRK3}$ and $Glu103^{CRK3}$ (Figure 7B), which is not possible in the
611 human CDK2 homolog. The influence of this bonding interaction on the cavity size and
612 subsequently on the ligand affinity could explain the observed gain of selectivity of 6-BIO towards
613 CRK3. The above holds with the exception of 6-IIO, the bisubstituted 5-Me-6-BIO and the
614 acetoxime 6-BIA, for which energy optimization calculations demonstrated that the presence of the
615 bulky substituent provoked a displacement of the ligand and the pair of residues Tyr101-Glu103
616 (Figure 7C) resulting in less favorable interactions and loss of affinity.
617 All aforementioned structural observations are in accordance with previous studies showing that
618 minor differences of the kinase binding cavity elements induce major variations in affinity and
619 should be taken into account in designing new selective inhibitors of the leishmanial GSK-3s and
620 CRK3. One possible route of selectively improving affinity towards the parasite GSK-3 is by taking

621 advantage of the differential presence of the proton accepting His155^{LGSK-3} (instead of Gln185$^{hGSK-3\beta}$ of human). The replacement or extension of the oxime by a group with the potential to form attractive albeit selective interactions with the sidechain of His155 $^{LGSK-3}$ would increase affinity towards the parasite protein. Combined with the obvious preference of *Ld*GSK-3 for bisubstituted or generally bulkier substituents with regard to CRK3, a moderate selectivity improvement can be achieved, resulting in an increase of parasite killing while reducing toxicity to human cells.

4. Discussion

Herein we showed that three 6-bromo substituted indirubins, 6-BIO, 6-BIA and 5-Me-6-BIO were powerful inhibitors of both *L. donovani* promastigote and intracellular amastigote growth. *L. donovani* axenic amastigotes were also inhibited by the three indirubins with IC_{50} values ≤ 1 μM, a finding that further supports that indirubin-induced growth inhibition of intracellular amastigotes is mediated through parasite-kinase(s) inhibition and not through inhibition of the host-kinase(s).

The adapted Alamar blue assay allows the rapid and easy screening of the antileishmanial activity of compounds in 96-well format, although it is not very quantitative for measuring intramacrophage *Leishmania* growth when compared to luciferase-expressing recombinant parasites (Roy et al., 2000). Also it does not measure the number of amastigotes at the point of lysis. However, contrary to Giemsa staining it takes into account only viable cells.

Since 6-bromo substitution on the indirubin backbone enhances the selectivity for mammalian GSK-3 over CDKs (Meijer et al., 2003) we investigated whether 6-BIO, 6-BIA and 5-Me-6-BIO target GSK-3 in *Leishmania a*nd studied their selectivity over CRK3. To this end we identified and characterized one of the two GSK-3 forms in *L. donovani*, namely *Ld*GSK-3s, and found that its expression pattern was comparable in logarithmic and stationary-phase promastigotes, but it was about 3-fold down-regulated in amastigotes, consistent with recent findings on *Ld*GSK-3s expression in *L. donovani* axenic amastigotes (Rosenzweig et al., 2008). In addition, *Ld*GSK-3s

647 which had cytosolic and flagellar localization in logarithmic-phase promastigotes, displayed nuclear
648 translocation in stationary-phase promastigotes. In mammalian cells, GSK-3β is also predominately
649 in the cytosol although under proapoptotic stimuli, a portion of GSK-3β is found within the nucleus
650 (Meares and Jope, 2007)**.** *Ld*GSK-3s translocation to the nucleus in stationary-phase promastigotes,
651 thought to be arrested in G1 phase of the cell-cycle (Wiesgigl and Clos, 2001), may reflect a role for
652 *Ld*GSK-3s in G1, consistent with accumulation of parasites in G1 when *Ld*GSK-3s is inhibited with
653 5-Me-6-BIO. The observed differences in the localization and expression level of *Ld*GSK-3s may
654 reflect divergent roles played by *Ld*GSK-3s in the two parasite stages. It could be speculated that in
655 the intracellular amastigotes the function of *Ld*GSK-3s may be linked among others to their
656 response and adaptation to stress conditions i.e. pH and temperature changes (Richard et al., 2005).
657 The finding that the level of inhibition of promastigotes and amastigotes by 5-Me-6-BIO is the
658 same although *Ld*GSK-3s is 3-fold less in amastigotes may suggest that *Ld*GSK-3s activity is
659 higher in the latter or that 5-Me-6-BIO may also target other kinases in this stage.
660 Inhibitor screen assays against *Ld*GSK-3s and CRK3 showed that 5-Me-6-BIO, which is a 50-
661 fold selective inhibitor of mammalian GSK-3 over CDK1/Cyclin B (Meijer et al., 2003;
662 Polychronopoulos et al., 2004) displayed an approximately 7-fold selectivity for *Ld*GSK-3s over
663 CRK3. However, 6-BIO was about 7-fold more active towards CRK3 than *Ld*GSK-3s, although it is
664 a mammalian GSK-3 selective inhibitor, with 64-fold less potency towards CDK1/Cyclin B
665 (Meijer et al., 2003). Molecular docking of the compounds in hGSK-3 and CDK1 active sites as
666 compared to *Ld*GSK-3s and CRK3 support the higher inhibitory activity of 5-Me-6-BIO towards
667 *Ld*GSK-3s compared to CRK3 and the lower inhibitory activity of 6-BIO towards *Ld*GSK-3s
668 compared to that against its mammalian counterpart.
669 5-Me-6-BIO and 6-BIO displayed a disparity between cellular activity and enzyme activity (Ki
670 values) (22-27 fold for 5-Me-6-BIO and 75-80 fold for 6-BIO), which can be attributed to: a) the
671 ATP concentration in the kinase assays, that is several fold lower than the intracellular
672 concentration, which is in the mM range, b) the bioavailability of the inhibitors (cell permeability of

673 the compounds, rate of inhibitor efflux by cell efflux pumps), c) possible *in vivo* phosphatase
674 activity, d) the intracellular concentration of the target kinase, e) the presence of the *Ld*GSK-3l
675 isoform and f) need for total inhibition of the enzyme to get cellular effect (Knight and Shokat,
676 2005).

677 We next investigated the effects on cell-cycle progression and the death process induced by 5-
678 Me-6-BIO treatment, using a number of different techniques. Its effect on parasite growth appeared
679 to be more dose- than time-dependent, as the IC_{50} values did not significantly vary with the
680 incubation time. However, 5-Me-6-BIO treatment affected the recovery potential of treated cells
681 after removal of the drug, as cells were able to recover after 48 h of treatment, whereas 72 h of
682 treatment caused an irreversible inhibition of cell growth .

683 In an effort to elucidate whether 5-Me-6-BIO targets *Ld*GSK-3s *in vivo* and the potential role of
684 *Ld*GSK-3s in cell-cycle progression and apoptosis-like death a sat-*Ld*GSK-3s over-expressor
685 mutant and a cell line expressing a kinase-dead mutant sat-*Ld*GSK-3s/K49R were generated. Cells
686 that over-express *Ld*GSK-3s (about 2-fold) were about 2-fold less susceptible to growth inhibition
687 than sat-*Ld*GSK-3s/K49R and sat transfectants at all time-points, indicating that the observed
688 growth inhibition was closely associated with inhibition of *Ld*GSK-3s activity by 5-Me-6-BIO. In
689 addition these results imply that the wild-type kinase should be inhibited by 5-Me-6-BIO with an
690 IC50 value comparable with that of the His-tagged *Ld*GSK-3s. Also, the 2-fold increase in *Ld*GSK-
691 3s expression in sat-*Ld*GSK-3s transfectants completely reversed the cell-cycle disruption effect of
692 5-Me-6-BIO and abolished the induction of apoptosis-like death. However, the *Ld*GSK-3s/K49R
693 expression resulted in similar phenotypes with those of the sat transfectants. The results provide
694 strong evidence that *Ld*GSK-3s is the intracellular target of 5-Me-6-BIO and suggest the direct or
695 indirect involvement of *Ld*GSK-3s in cell-cycle control as well as in pathways leading to apoptosis-
696 like death. Although there is evidence that apoptosis-like death occurs in *Leishmania* (Das et al.,
697 2001) the pathways and proteins involved remain to be elucidated. GSK3 is known to modulate
698 apoptosis in mammalian cells, by regulating the apoptotic pathways (Beurel and Jope, 2006).

699 Therefore common pathways may exist between *Leishmania* and mammalian cells in regulating
700 apoptotic signaling pathways through GSK-3.

701 In contrast to 5-Me-6-BIO, 6-BIO induced a time-dependent growth inhibition accompanied
702 with a dose- and time-dependent accumulation of cells in G2/M. Moreover, 6-BIO induced
703 apoptosis-like death in a lower proportion of promastigotes compared to 5-Me-6-BIO and this death
704 process progressed more slowly in parasites exposed to 6-BIO. These differences between the
705 cellular effects induced by 6-BIO compared to 5-Me-6-BIO suggest that *in vivo* the two indirubins
706 may target different kinases and/or pathways.

707 The observation that over-expression of *Ld*GSK-3s only partially reversed the effect of 6-BIO is
708 not unexpected, since *in vitro* 6-BIO preferentially inhibits CRK3. Moreover, the phenotype of
709 promastigotes incubated with 6-BIO, especially the accumulation of cells in G2/M, is consistent
710 with inhibition of CRK3, which is essential for cell-cycle progression at the G2/M phase transition
711 (Grant et al., 1998; Hassan et al., 2001) and implies that CRK3 may be the main intracellular target
712 of 6-BIO. Although 6-BIO was a more effective inhibitor of CRK3, and despite the observed
713 phenotype being consistent with CRK3-inhibition, the fact that *Ld*GSK-3s over-expression partially
714 reversed promastigote G2/M arrest and partially protected cells from 6-BIO induced apoptosis-like
715 death, implies that 6-BIO may also target *Ld*GSK-3s in the parasite where the level of expression of
716 the two kinases is not known. Since 6-BIO arrests promastigotes in G2/M phase of the cell-cycle,
717 this may mean that *Ld*GSK-3s also plays a role in G2/M phase transition, although this is difficult to
718 reconcile with the results for 5-Me-6-BIO. Alternatively, over-expression of *Ld*GSK-3s may
719 influence 6-BIO activity by a non-specific mechanism (i.e. lower proportion of 6-BIO available for
720 binding to and inactivating CRK3).

721 In conclusion, the complete reversal of the cellular effects induced by 5-Me-6-BIO in the over-
722 expressing parasites strongly implies that *Ld*GSK-3s is the main target of 5-Me-6-BIO and suggests
723 a potential role for *Ld*GSK-3s in cell-cycle progression and in apoptosis-like death. Moreover, the
724 dramatic effect of *Ld*GSK-3s inhibitors on *Leishmania*, especially the intramacrophage amastigote

stage, suggests that *Ld*GSK-3s has potential as a drug target in these parasites. Future work would be required to develop parasite-selective inhibitors that do not target host GSK-3 since its inhibition may affect the balance between Th1 and Th2 rsponses (Ohtani et al., 2008). In addition, RNAi studies of *Tbru*GSK-3 lead to similar cellular phenotypes, such as growth inhibition and altered parasite morphology (Ojo et al., 2008), to that caused by GSK-3 inhibitors in *Leishmania*. Importantly, the very recent validation of *Tbru*GSK-3 as a drug target for this protozoan parasite too (Ojo et al., 2008), reinforces our claim that GSK-3 could constitute a trans-trypanosomatid as well as trans-protozoan target, including *P. falciparum* and that it should be exploited for anti-protozoan drug development.

Acknowledgements. This work was supported by HPI (E.X. PhD fellowship), by the General Secretariat of Research and Technology of Greece; PENED program (V.M.), University of Athens program Kapodistrias and by the FP6-2002-Life Sciences & Health, PRO-KINASE Research Project (LM). We thank our colleagues Dr. Christos Haralambous for the generation of the phylogenetic tree and Georgia Konidou for technical assistance.

References

Alvar, J., Yactayo, S., Bern, C., 2006. Leishmaniasis and poverty. Trends Parasitol 22, 552-557.

Barak, E., Amin-Spector, S., Gerliak, E., Goyard, S., Holland, N., Zilberstein, D., 2005. Differentiation of Leishmania donovani in host-free system: analysis of signal perception and response. Mol Biochem Parasitol 141, 99-108.

Beurel, E., Jope, R.S., 2006. The paradoxical pro- and anti-apoptotic actions of GSK3 in the intrinsic and extrinsic apoptosis signaling pathways. Prog Neurobiol 79, 173-189.

Bohmer, F.D., Karagyozov, L., Uecker, A., Serve, H., Botzki, A., Mahboobi, S., Dove, S., 2003. A single amino acid exchange inverts susceptibility of related receptor tyrosine kinases for the ATP site inhibitor STI-571. J Biol Chem 278, 5148-5155.

Chang, K.P., 1983. Cellular and molecular mechanisms of intracellular symbiosis in leishmaniasis. Int Rev Cytol Suppl 14, 267-305.

Croft, S.L., Sundar, S., Fairlamb, A.H., 2006. Drug resistance in leishmaniasis. Clin Microbiol Rev 19, 111-126.

Damiens, E., Baratte, B., Marie, D., Eisenbrand, G., Meijer, L., 2001. Anti-mitotic properties of indirubin-3'-monoxime, a CDK/GSK-3 inhibitor: induction of endoreplication following prophase arrest. Oncogene 20, 3786-3797.

Das, M., Mukherjee, S.B., Shaha, C., 2001. Hydrogen peroxide induces apoptosis-like death in Leishmania donovani promastigotes. J Cell Sci 114, 2461-2469.

Davies, T.G., Tunnah, P., Meijer, L., Marko, D., Eisenbrand, G., Endicott, J.A., Noble, M.E., 2001. Inhibitor binding to active and inactive CDK2: the crystal structure of CDK2-cyclin A/indirubin-5-sulphonate. Structure 9, 389-397.

Doble, B.W., Woodgett, J.R., 2003. GSK-3: tricks of the trade for a multi-tasking kinase. J Cell Sci 116, 1175-1186.

Dujardin, J.C., 2006. Risk factors in the spread of leishmaniases: towards integrated monitoring? Trends Parasitol 22, 4-6.

Frame, S., Cohen, P., Biondi, R.M., 2001. A common phosphate binding site explains the unique substrate specificity of GSK3 and its inactivation by phosphorylation. Mol Cell 7, 1321-1327.

Grant, K.M., Hassan, P., Anderson, J.S., Mottram, J.C., 1998. The crk3 gene of Leishmania mexicana encodes a stage-regulated cdc2-related histone H1 kinase that associates with p12. J Biol Chem 273, 10153-10159.

Grant, K.M., Dunion, M.H., Yardley, V., Skaltsounis, A.L., Marko, D., Eisenbrand, G., Croft, S.L., Meijer, L., Mottram, J.C., 2004. Inhibitors of Leishmania mexicana CRK3 cyclin-dependent kinase: chemical library screen and antileishmanial activity. Antimicrob Agents Chemother 48, 3033-3042.

Habtemariam, S., 2003. In vitro antileishmanial effects of antibacterial diterpenes from two Ethiopian Premna species: P. schimperi and P. oligotricha. BMC Pharmacol 3, 6.

Hanks, S.K., Quinn, A.M., 1991. Protein kinase catalytic domain sequence database: identification of conserved features of primary structure and classification of family members. Methods Enzymol 200, 38-62.

Hassan, P., Fergusson, D., Grant, K.M., Mottram, J.C., 2001. The CRK3 protein kinase is essential for cell cycle progression of Leishmania mexicana. Mol Biochem Parasitol 113, 189-198.

He, X., Saint-Jeannet, J.P., Woodgett, J.R., Varmus, H.E., Dawid, I.B., 1995. Glycogen synthase kinase-3 and dorsoventral patterning in Xenopus embryos. Nature 374, 617-622.

Hoessel, R., Leclerc, S., Endicott, J.A., Nobel, M.E., Lawrie, A., Tunnah, P., Leost, M., Damiens, E., Marie, D., Marko, D., Niederberger, E., Tang, W., Eisenbrand, G., Meijer, L., 1999. Indirubin, the active constituent of a Chinese antileukaemia medicine, inhibits cyclin-dependent kinases. Nat Cell Biol 1, 60-67.

Ilg, T., 2002. Generation of myo-inositol-auxotrophic Leishmania mexicana mutants by targeted replacement of the myo-inositol-1-phosphate synthase gene. Mol Biochem Parasitol 120, 151-156.

Knight, Z.A., Shokat, K.M., 2005. Features of selective kinase inhibitors. Chem Biol 12, 621-637.

Laskowski, R., MacArthur, M., Moss, D., Thornton, J., 1991. PROCHECK: A programm to check the stereochemichal quality of protein structures. J. Appl. Crystallogr. 26, 283-291.

Meares, G.P., Jope, R.S., 2007. Resolution of the nuclear localization mechanism of glycogen synthase kinase-3: functional effects in apoptosis. J Biol Chem 282, 16989-17001.

Meijer, L., Skaltsounis, A.L., Magiatis, P., Polychronopoulos, P., Knockaert, M., Leost, M., Ryan, X.P., Vonica, C.A., Brivanlou, A., Dajani, R., Crovace, C., Tarricone, C., Musacchio, A., Roe, S.M., Pearl, L., Greengard, P., 2003. GSK-3-selective inhibitors derived from Tyrian purple indirubins. Chem Biol 10, 1255-1266.

Meijer, L., Flajolet, M., Greengard, P., 2004. Pharmacological inhibitors of glycogen synthase kinase 3. Trends Pharmacol Sci 25, 471-480.

Mikus, J., Steverding, D., 2000. A simple colorimetric method to screen drug cytotoxicity against Leishmania using the dye Alamar Blue. Parasitol Int 48, 265-269.

Naula, C., Parsons, M., Mottram, J.C., 2005. Protein kinases as drug targets in trypanosomes and Leishmania. Biochim Biophys Acta 1754, 151-159.

Ohtani, M., Nagai, S., Kondo, S., Mizuno, S., Nakamura, K., Tanabe, M., Takeuchi, T., Matsuda, S., Koyasu, S., 2008. Mammalian target of rapamycin and glycogen synthase kinase 3 differentially regulate lipopolysaccharide-induced interleukin-12 production in dendritic cells. Blood 112, 635-643.

Ojo, K.K., Gillespie, J.R., Riechers, A.J., Napuli, A.J., Verlinde, C.L., Buckner, F.S., Gelb, M.H., Domostoj, M.M., Wells, S.J., Scheer, A., Wells, T.N., Van Voorhis, W.C., 2008. Glycogen Synthase Kinase 3 is a Potential Drug Target for African Trypanosomiasis Therapy. Antimicrob Agents Chemother.

Papageorgiou, F.T., Soteriadou, K.P., 2002. Expression of a novel Leishmania gene encoding a histone H1-like protein in Leishmania major modulates parasite infectivity in vitro. Infect Immun 70, 6976-6986.

Parsons, M., Worthey, E.A., Ward, P.N., Mottram, J.C., 2005. Comparative analysis of the kinomes of three pathogenic trypanosomatids: Leishmania major, Trypanosoma brucei and Trypanosoma cruzi. BMC Genomics 6, 127.

Polychronopoulos, P., Magiatis, P., Skaltsounis, A.L., Myrianthopoulos, V., Mikros, E., Tarricone, A., Musacchio, A., Roe, S.M., Pearl, L., Leost, M., Greengard, P., Meijer, L., 2004. Structural basis for the synthesis of indirubins as potent and selective inhibitors of glycogen synthase kinase-3 and cyclin-dependent kinases. J Med Chem 47, 935-946.

Ribas, J., Garrofe-Ochoa, X., Boix, J., 2006. Characterization of the cell death processes triggered by indirubin derivatives in neuroblastoma cells
In: Meijer, L., Guyard, N., Skaltsounis, L. A., Eisenbrand, G (Ed.), Indirubin, the red shade of indigo, Life in Progress Editions, Roscoff, France, pp. 215-226.

Richard, O., Paquet, N., Haudecoeur, E., Charrier, B., 2005. Organization and expression of the GSK3/shaggy kinase gene family in the moss Physcomitrella patens suggest early gene multiplication in land plants and an ancestral response to osmotic stress. J Mol Evol 61, 99-113.

Rosenzweig, D., Smith, D., Opperdoes, F., Stern, S., Olafson, R.W., Zilberstein, D., 2008. Retooling Leishmania metabolism: from sand fly gut to human macrophage. Faseb J 22, 590-602.

Roy, G., Dumas, C., Sereno, D., Wu, Y., Singh, A.K., Tremblay, M.J., Ouellette, M., Olivier, M., Papadopoulou, B., 2000. Episomal and stable expression of the luciferase reporter gene for quantifying Leishmania spp. infections in macrophages and in animal models. Mol Biochem Parasitol 110, 195-206.

Sali, A., Blundell, T.L., 1993. Comparative protein modelling by satisfaction of spatial restraints. J Mol Biol 234, 779-815.

Smirlis, D., Bisti, S.N., Xingi, E., Konidou, G., Thiakaki, M., Soteriadou, K.P., 2006. Leishmania histone H1 overexpression delays parasite cell-cycle progression, parasite differentiation and reduces Leishmania infectivity in vivo. Mol Microbiol 60, 1457-1473.

Stewart, J.J., 1990. MOPAC: a semiempirical molecular orbital program. J Comput Aided Mol Des 4, 1-105.

Wells, C., McNae, I., Walkinshaw, M., Westwood, N.J., Grant, K.M., 2006. The selective biological activity of indirubin-based inhibitors: applications in parasitology. In: Meijer, L., Guyard, N., Skaltsounis, L. A., Eisenbrand, G (Ed.), Indirubin, the red shade of indigo, Life in Progress Editions, Roscoff, France, pp. 259-267.

Wiesgigl, M., Clos, J., 2001. Heat shock protein 90 homeostasis controls stage differentiation in Leishmania donovani. Mol Biol Cell 12, 3307-3316.

FIGURE LEGENDS

Fig 1. *Ld*GSK-3s expression in *L. donovani*: Western blot analysis (A) anti-*Ld*GSK-3s antibody: Stationary-phase promastigotes (S), logarithimic-phase promastigotes (L), axenic amastigotes (Ax), spleen-derived amastigotes (Am) and J774 macrophages (J774) 10^7 parasites or 9×10^5 macrophage cells were loaded per lane. (B) anti-*Lin*INO1 antibody, to confirm equal cell loading. (C) Pre-immune serum: Stationary-phase promastigotes (S) and axenic amastigotes (Ax). (D) anti-ratGSK-3β antibody: Stationary-phase promastigotes (10^7) and J774 cell extracts (9×10^5 cells/lane), used as positive controls. Evaluation of the level of expression of *Ld*GSK-3s was analyzed using the Alpha Imager Software and compared to that of INO1. (E) Localization of *Ld*GSK-3s in *L. donovani* logarithmic and stationary-phase promastigotes and logarithmic-phase axenic amastigotes, using the affinity-purified anti-*Ld*GSK-3s antibody (5 μg/ml). Parasite nuclei and kinetoplasts were counterstained with PI. Scale bars 4 μm.

Fig 2. Kinase activity of *Ld*GSK-3s purified from *L. donovani* over-expressing transfectants. The ability of *Ld*GSK-3s (1 μg *Ld*GSK-3s/reaction) to phosphorylate various substrates was assessed *in vitro*. Kinase reactions, containing approximately 1 μg substrate/reaction, were subjected to SDS-PAGE and phosphorylated substrates detected by autoradiography. Lane 1, *Ld*GSK-3s; lane 2, LeishH1**;** lane 3, LeishH1 plus 4 μM 5-Me-6-BIO; lane 4, LeishH1 plus kinase-dead *Ld*GSK-3s/K49R; lane 5, GST; lane 6, axin; lane 7, myelin basic protein, MBP; lane 8, mammalian histone H1 and lane 9, casein.

Fig 3. Effects of indirubins on cell-cycle progression and apoptosis-like cell death. Flow cytometry was used to assess the cell-cycle status of *L. donovani* promastigotes exposed to indirubins *in vitro* (A) Stationary-phase promastigotes were seeded at 1 x 10^6 cells/ml and incubated in the presence of 5-Me-6-BIO (1 μM or 2 μM) or DMSO (control), for 24 h or 48 h or (B) 6-BIO (1 μM or 2 μM) or DMSO (control), for 24 h or 48 h. (C) *L. donovani* promastigotes were incubated with 2 μM 5-Me-

885 6-BIO, 2 μM 6-BIO or DMSO (Control) for 48 h and then stained with Annexin V-FITC and PI to
886 assess phosphatidylserine translocation and membrane integrity. Promastigotes were also incubated
887 with either 4 mM H_2O_2 for 40 min (apoptosis positive control) or 0.1% Triton X-100 for 5 min
888 (necrosis positive control). Flow cytometry was performed using a FACSCalibur and data analyzed
889 using the Cell Quest software. The percentage of cells in each quadrant represent the following:
890 lower left, double negative; upper left, PI single positive; lower right, Annexin V single positive and
891 upper right, PI-Annexin V double positive. Results are representative of three independent
892 experiments. (D) *L. donovani* promastigotes were incubated with 2 μM 5-Me-6-BIO for 24h, 48 h
893 and 72 h. At these time-points (white bars/0 h), drug was removed followed by further incubation of
894 cells in drug-free medium for 24 h (black bars),, 48 h (gray bars) and 72 h (dotted bars). The
895 percentages of cell viability were determined using the trypan blue exclusion test. Error bars
896 represent the standard deviations of three independent experiments.
897
898 **Fig. 4**. Cell and nuclear morphology of *L. donovani* promastigotes exposed to indirubins: *L.*
899 *donovani* promastigotes were incubated with 2 μM 5-Me-6-BIO, 2 μM 6-BIO or 0.02% DMSO
900 (control) for 24 and 48 hours, *in vitro*, and then fixed and stained with propidium iodide. Confocal
901 micrographs are representative of three independent experiments. Scale bar 4 μm. N, nucleus; K,
902 kinetoplast; white arrows indicate condensed nuclei; blue arrows indicate disintegrated nuclei.
903
904 **Fig. 5**. Over-expression of *Ld*GSK-3s counteracts the effects of 5-Me-6-BIO and 6-BIO on *L.*
905 *donovani* promastigotes: (A) Western blot analysis of *L. donovani* sat, sat-*Ld*GSK-3s/K49R and sat-
906 *Ld*GSK-3s promastigotes (10^7/lane) probed with His-probe, anti-*Ld*GSK-3s or anti-*Lin*INO1
907 antibodies. The intensity of the bands was analyzed with the use of the Alpha Imager Software and
908 the fold-over-expression estimated. (B) Growth inhibition of *L. donovani* sat (gray symbols, dotted
909 lines), sat-*Ld*GSK-3s/K49R (solid symbols) and sat-*Ld*GSK-3s (open symbols) transfectants treated
910 with different 5-Me-6-BIO concentrations after 24 h, 48 h and 72 h of incubation. Results are

depicted from four independent experiments performed in duplicate. (C) Flow cytometry analysis of *L. donovani* sat, sat-*Ld*GSK-3s/K49R and sat-*Ld*GSK-3s transfectants incubated in the presence of 0.02% DMSO (control) or 2 μM 5-Me-6-BIO or 2 μM 6-BIO for 48 h. Results are indicative of three independent experiments. (D) Growth inhibition of *L. donovani* sat (gray symbols, dotted lines), sat-*Ld*GSK-3s/K49R (solid symbols) and sat-*Ld*GSK-3s (open symbols) transfectants treated with different 6-BIO concentrations after 24 h, 48 h and 72 h of incubation. Results are depicted from four independent experiments performed in duplicate.

Fig. 6. DNA fragmentation in *L. donovani* promastigotes incubated with indirubins: *L. donovani* sat, sat-*Ld*GSK-3s/K49R and sat-*Ld*GSK-3s transfectants were incubated with 0.02% DMSO (negative control), 2 μM 5-Me-6-BIO, 2 μM 6-BIO or 4mM H_2O_2 (apoptosis positive control) and then subjected to TUNEL-labeling. Cells were visualized under a Zeiss fluorescence microscope at 120× magnification. The experiment was performed three times.

Fig. 7 (A) A superposition of the crystal structure of human GSK3 active site complexed with 6-BIO (green) and the complex of *Ld*GSK3s-6-BIO resulting from docking calculations (turquoise). Hydrogen bonds are depicted as yellow dotted lines. Residues within the active site which differ between human and *L. donovani* GSK3s are annotated, with the most important for 6-BIO affinity being the gatekeeper mutation of leucine132 in the human to methionine100 in the parasite protein. (B) Overlay of the crystal structure of CDK2 complexed with indirubin-5-sulphonate (turquoise) and the CRK3 homology model (orange). The double mutation of $phe82^{CDK2}$ to tyr101 and of $his84^{CDK2}$ to glu103 results in a hydrogen bond between tyrosine and glutamate (shown in yellow) that translates the paired sidechains towards the cavity reducing its volume and offering a rigid partner for stacking or charge dipole stabilizing interactions with the extended aromatic scaffold of indirubins to form. (C) Ligands 6-BIO (green) and 5-Me-6-BIO (orange) in the CRK3 binding

936 cavity as resulted from simple energy minimizations. Visible are the displacements of the
937 bisubstituted 5-Me-6-BIO relative to 6-BIO and of the tyrosine-glutamate bonded pair.
938

TABLES

Table 1: Indirubin compounds tested *in vitro* for their antileishmanial activity against *L. donovani* promastigotes (P), intracellular amastigotes (In. A) and axenic amastigotes (Ax. A) using the Alamar blue assay.

Indirubin-backbone showing possible substitutions at positions 3', 5, 6 and N_1 (Y, W, X and R respectively)

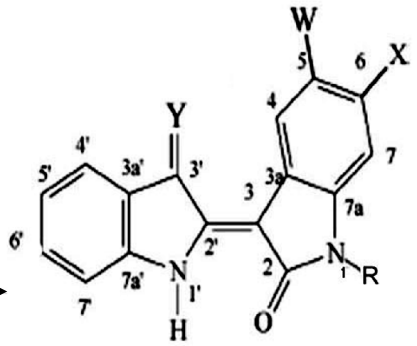

Compounds	Y	X	W	R	*L. donovani* P	*L. donovani* In. A	*L. donovani* Ax. A
					IC_{50} (µM)*		
Indirubin	O	H	H	H	n.i.†	n.i.	n.i.
Indirubin-3'oxime	NOH	H	H	H	n.i.	n.i.	n.i.
5-Br-indirubin	O	H	Br	H	n.i.	n.i.	n.i.
5-Br-indirubin-3'oxime (5-BIO)	NOH	H	Br	H	5.2±1.6	1±0.15	1 ±0.2
5-aminoindirubin-3'oxime	NOH	H	NH_2	H	>10 ‡	>10	>10
6-Br-indirubin	O	Br	H	H	n.i.	n.i.	n.i.
6-Br-indirubin-3'oxime (6-BIO)	NOH	Br	H	H	0.8±0.1	0.75±0.05	0.9±0.1
6-Br-N-methyl-indirubin-3'-oxime	NOH	Br	Br	CH_3	n.i.	n.i.	n.i.
6-Br-indirubin-3'acetoxime (6-BIA)	NOAc	Br	H	H	0.9±0.1	1±0.05	1± 0.1
6-Br-N-methyl-indirubin-3'acetoxime	NOAc	Br	H	CH_3	n.i.	n.i.	n.i.
6-Br-indirubin-3'diethyl phosphatoxime	$NOPO(OEt)_2$	Br	H	H	>10	>10	>10
Indirubin-3'-methoxime	$NOCH_3$	H	H	H	n.i.	n.i.	n.i.
6-Br-5nitroindirubin	O	Br	NO_2	H	n.i.	n.i.	n.i.

6-Br-5nitroindirubin-3'-oxime	NOH	Br	NO_2	H	>10	>10	>10
6-Br-5methylindirubin	O	Br	CH_3	H	n.i.	n.i.	n.i.
6-Br-5methylindirubin-3'oxime (5-Me-6-BIO)	NOH	Br	CH_3	H	1.2±0.2	1±0.1	1±0.2

[*] IC_{50} values were determined from dose-response curves and are expressed in μM. [†] n.i., no inhibition at 50 μM. [‡] IC_{50} values ranging between 10 and 50 μM.

Table 2: Amino-acid identity (%, above diagonal) and similarity (%, below diagonal) relationships of *L. infantum* GSK-3 enzymes versus human and *T. brucei* proteins [*]

	***H.sap* GSK-3β**	***H.sap* GSK-3α**	***L.inf* GSK-3s**	***L.inf* GSK-3l**	***T.bru* GSK-3s**	***T.bru* GSK-3l**
***H.sap* GSK-3β**		67.1	39.5	22	40.7	32.2
***H.sap* GSK-3α**	74.4		34.3	21.5	35.4	30.5
***L.inf* GSK-3s**	55.8	48.1		19.5	65.4	29.8
***L.inf* GSK-3l**	30.5	30.6	29.2		20.1	26.5
***T.bru* GSK-3s**	55.9	48.1	80.6	27.9		31.2
***T.bru* GSK-3l**	47.8	45.7	43.1	36.4	44.7	

[*] The table was constructed using BioEdit 7.0.5.3 Sequence Alignment Editor (pairwise global alignments using BLOSUM62 similarity matrix). Accession numbers for the enzymes were: *H. sapiens* GSK-3β (**P49841**), *H. sapiens* GSK-3α (**P49840**), *L. infantum* GSK-3s (**XP_001464844,** LinJ18_V3.0270), *L. infantum* GSK-3l (**XP_001465568,** LinJ22_V3.0370), *T. brucei* GSK-3short (**Tb10.61.3140**), *T. brucei* GSK-3long (**Tb927.7.2420**).

Table 3: Inhibition of *Ld*GSK-3s and CRK3 kinase activities by indirubins*.

Compounds	**IC_{50} (µM)**	
	***Ld*GSK-3s**	**CRK3**
5-BIO	0.35	0.7
6-BIO	0.15	0.02
N-methyl-6-BIO	>10	>10
6-BIA	0.17	0.25
N-methyl-6-BIA	>10	>10
5-Me-6-BIO	0.09	0.65
6-FIO	3.3	0.4
6-ClIO	0.2	0.04
6-IIO	0.2	1

*_Ld_GSK-3s and CRK3 were assayed for their ability to phosphorylate GS-1 peptide and mammalian histone H1 respectively in the presence of increasing concentrations of compounds. IC_{50} values were determined from dose-response curves and are expressed in µM.

FIGURE 1

Click here to download high resolution image

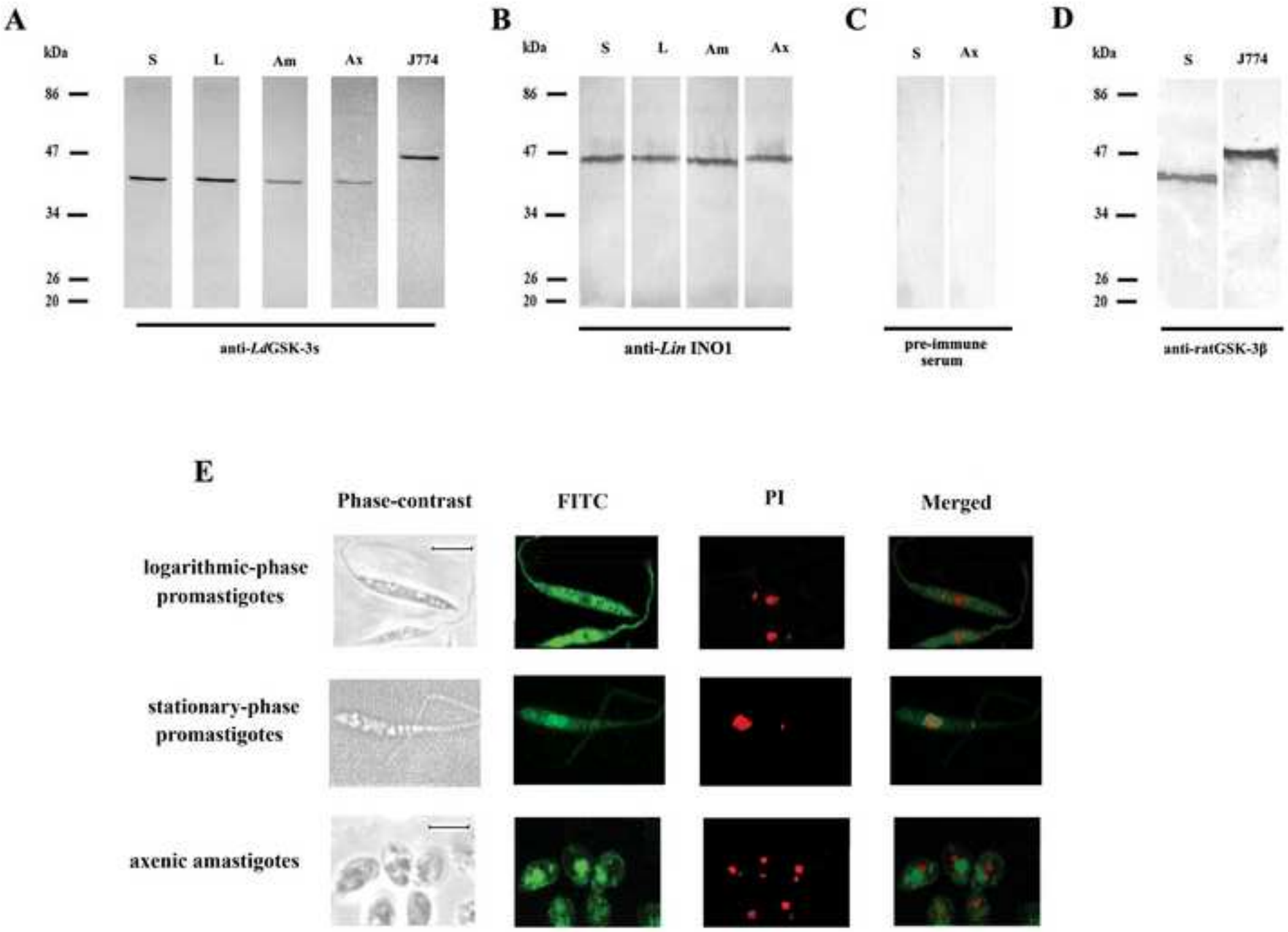

FIGURE 2

Click here to download high resolution image

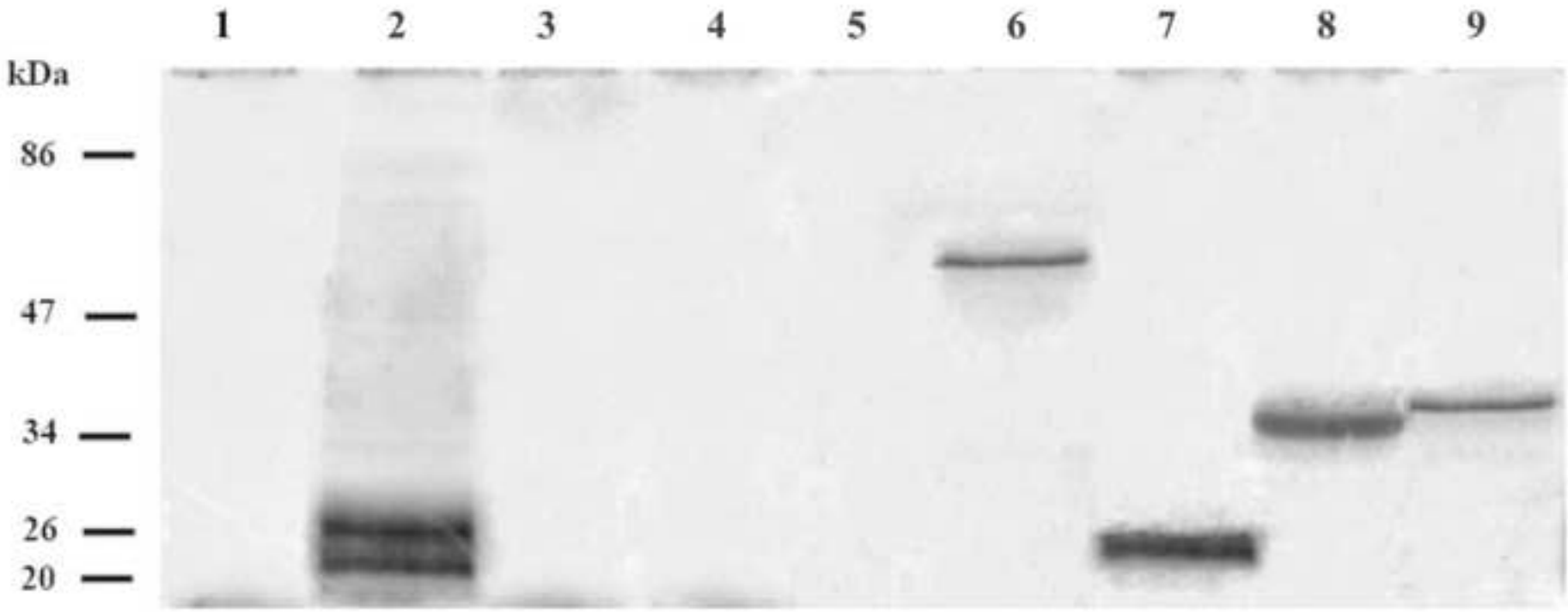

FIGURE 3

Click here to download high resolution image

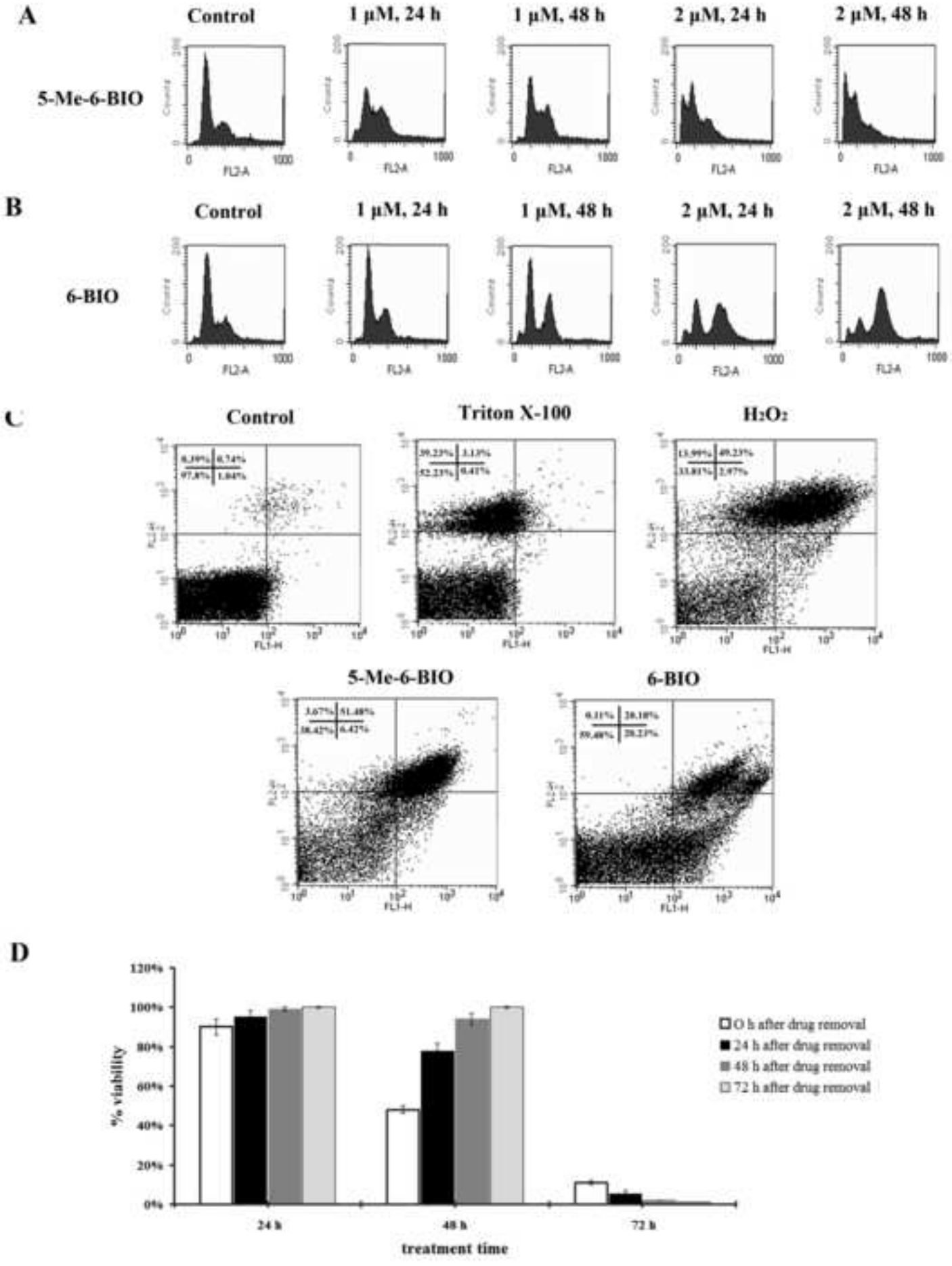

FIGURE 4

Click here to download high resolution image

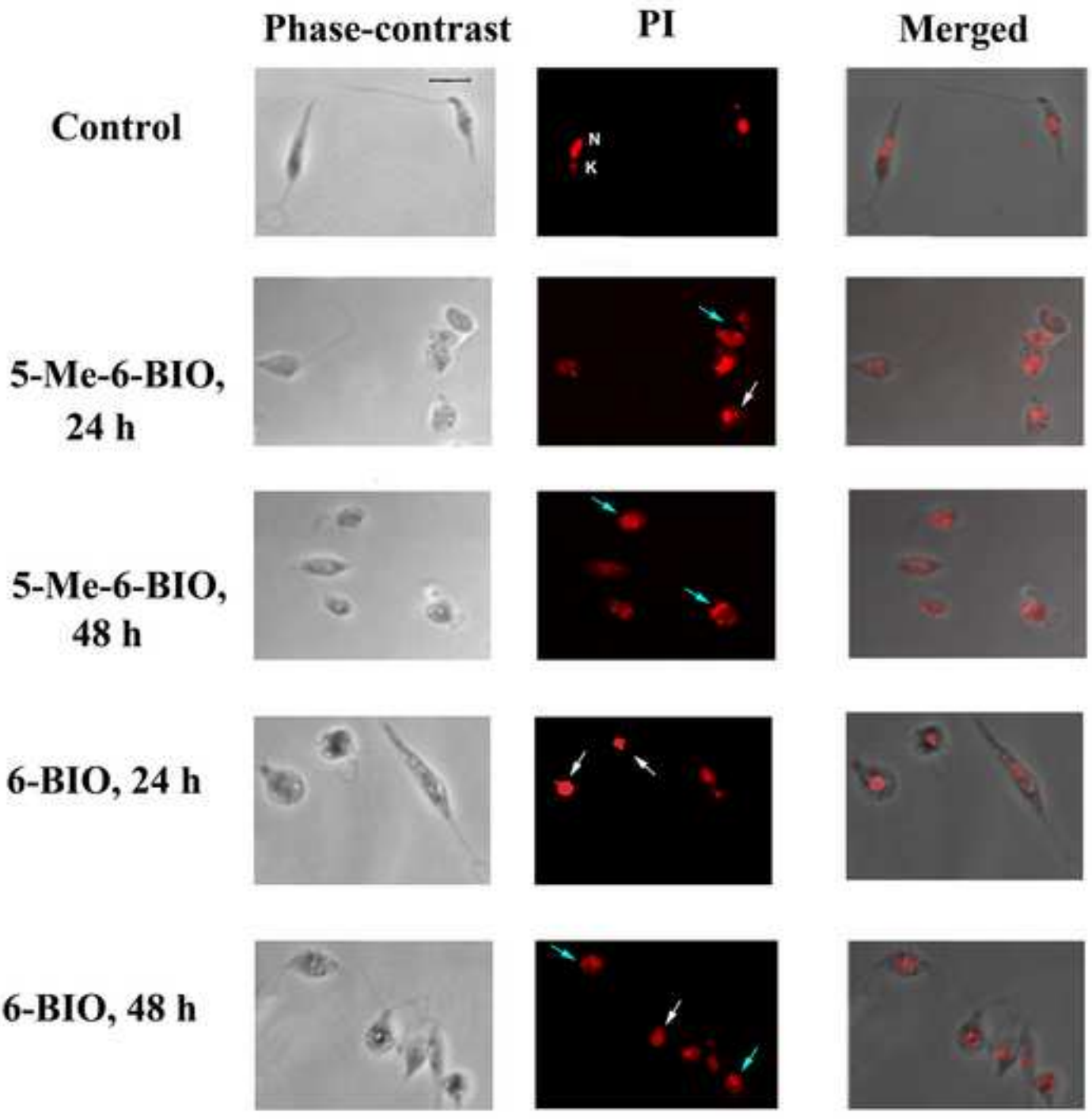

FIGURE 5

Click here to download high resolution image

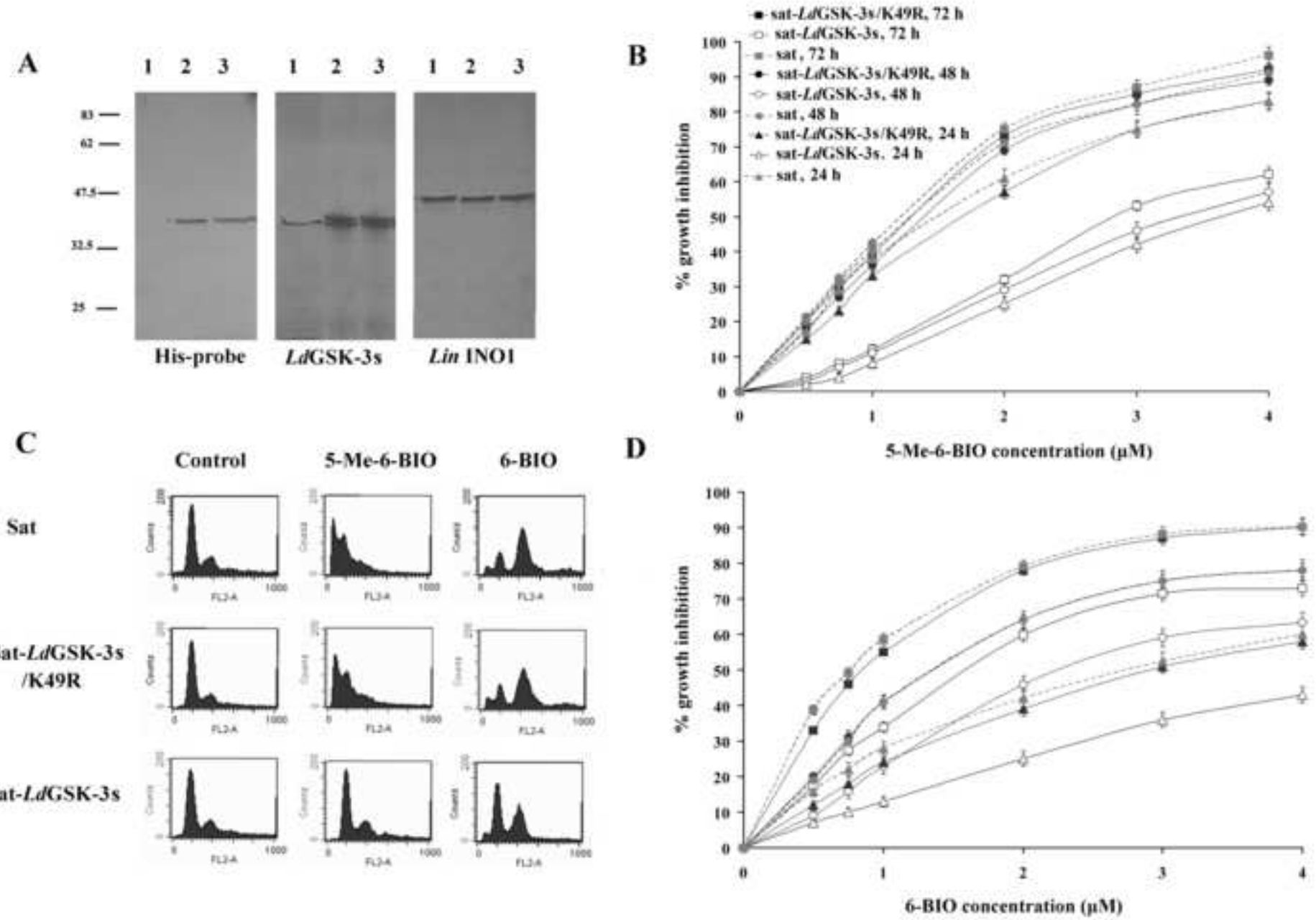

FIGURE 6

Click here to download high resolution image

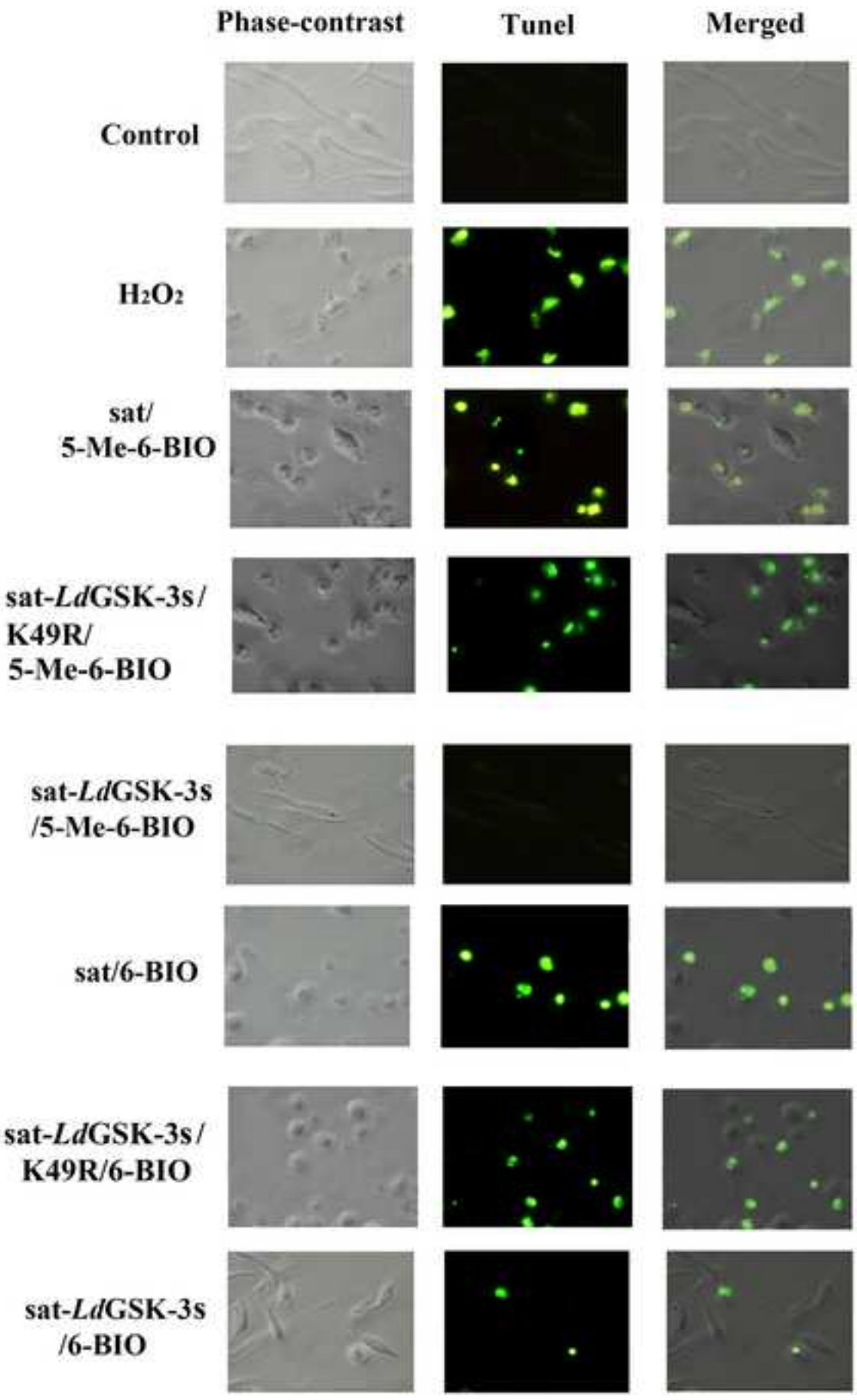

FIGURE 7

Click here to download high resolution image

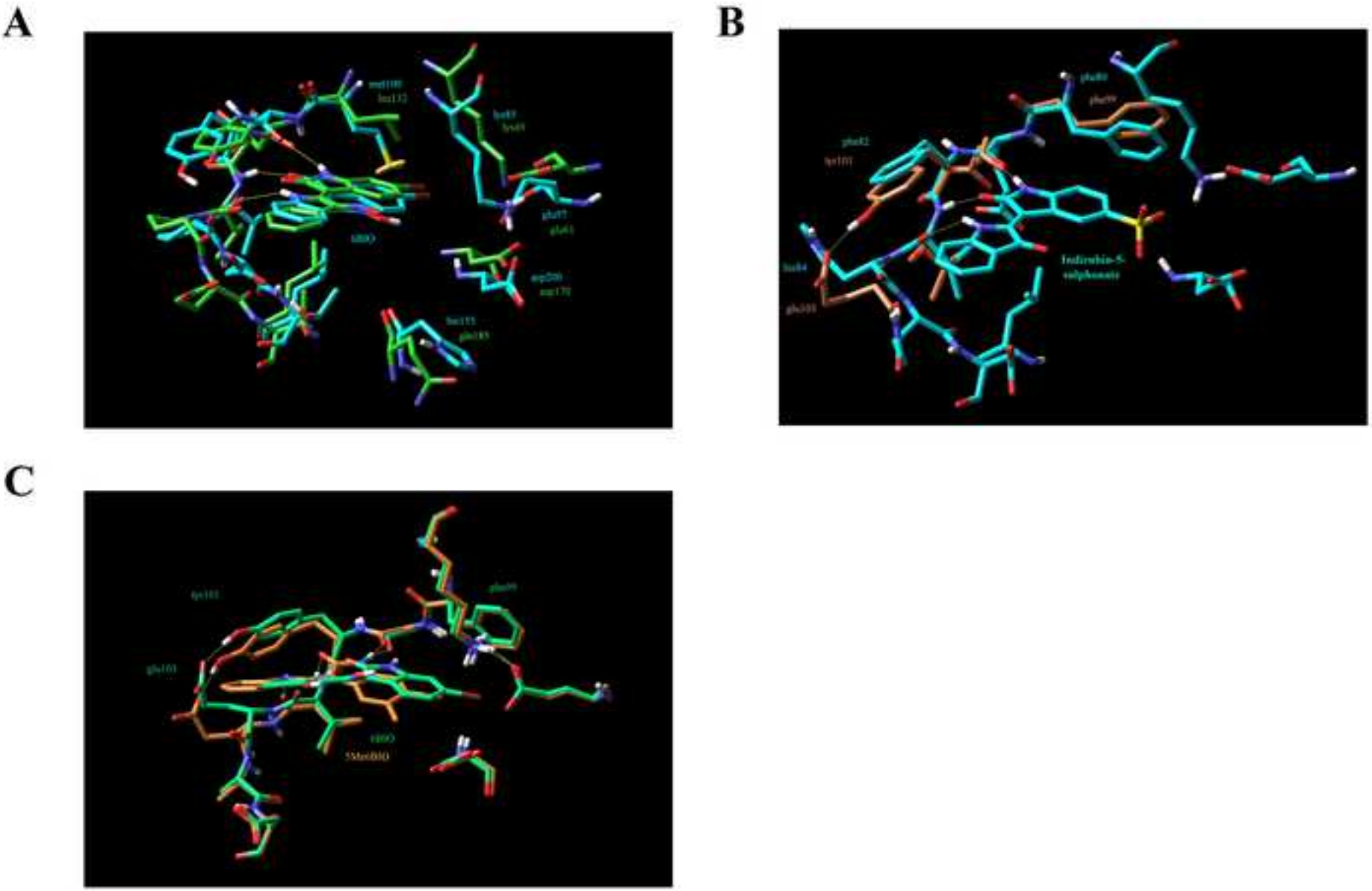

SUPPLEMENTARY DATA

Supplementary on Materials and Methods 2.13 (Homology modeling)

The sequence used for the construction of parasite GSK-3s structural model was expasy entry Q4QE15. The sequence used for CRK3 homology model was expasy entry O96526. Forty models were generated using the loop optimization routine and a slow simulated annealing refining protocol as implemented in MODELLER v.6 (Sali and Blundell, 1993) and each one was geometry optimized by subsequent steps of SD (50 steps) and PRCG (20000) minimizations with a restraining force on the protein α-carbons. The best model was chosen by a consensus of the program objective function and stereochemical scores obtained by PROCHECK (Laskowski, 1991). To check the stability of the final model, a Stochastic Dynamics simulation of 100ps equilibration and 400ps productive run was performed using the SHAKE algorithm on all bonds. The RMSD of the enzyme α-carbons from starting coordinates was recorded as a function of time showing that the model is stable.

For the docking experiments, the inhibitors were manually docked in the model binding cavity and a first minimization was performed with force constraints on the three hydrogen bonds formed between each indirubin and the kinase backbone in their crystallographic distances and angles as they appear in the reference crystal structure of 6-BIO with human GSK-3β (1UV5). A 1000 steps Monte Carlo local search of each inhibitor-protein complex followed, where all residues within 6Å from the ligand were free to move except Arg109. In the contracted binding pocket of the *L.major* GSK-3 apo crystal structure, inhibitors were fit by manually docking and performing short (300ps) MD runs instead of plain minimizations. The AMBER* (docking) or AMBER94 forcefields (dynamics) and the GB/SA continuum solvent model were used in all calculations as implemented in MACROMODEL v.9 (Mohamadi, 1990).

Supplementary on Results 3.3

Structurally divergent inhibitors

Structurally divergent inhibitors of mammalian GSK-3 and CDK were also tested on both *Ld*GSK-3s and CRK3 and their activity was lower than that of indirubins. These belonged to the following chemical families: benzazepinones (kenpaullone and alsterpaullone) pyrrolopyrazines (Aloisine A), pyrroloazepines (Hymenialdisine), maleimides (SB 216763 and SB 415286), thiadiazolidinones (TDZD-8) and aminothiazoles (SNS-032), (Coghlan et al., 2000; Leost et al., 2000; Meijer et al., 2000; Martinez et al., 2002; Mettey et al., 2003; Ali et al., 2007), (supplementary Table 1). More specifically, the activity of Kenpaullone on both kinases was low, while alsterpaullone was active towards *Ld*GSK-3s with an IC_{50} of 0.2 μM and inhibited parasite growth with an IC_{50} of 3.5 μM. The activity of Aloisine A on both kinases was also low, while Hymenialdisine was more selective for CRK3 and inhibited parasite growth with an IC_{50} of 5 μM. The maleimides SB 216763 and SB 415286 were active towards *Ld*GSK-3s and inactive on CRK3 and inhibited parasite growth with IC_{50} values of >5 μM. The only non-ATP competitive inhibitor tested, TDZD-8, as well as the CDK selective inhibitor SNS-032 were found to be completely inactive on both kinases.

Supplementary on Results 3.7

Homology modeling

The homology models of the parasite kinases were created as follows. CRK3 structural model was built on the template of the human CDK2-cyclinA complex (1E9H), (Davies et al., 2001). The leishmanial GSK-3 structural model was built on the human GSK-3-indirubin co-crystal structure (1UV5), although the crystal structure of leishmanial GSK-3 was recently deposited (pdb code 3E3P). In the crystal structure, the kinase was determined in its apoenzyme form, which is not considered as suitable for docking experiments as the corresponding holo structures (McGovern and Shoichet, 2003). In addition, the sequence similarity between the parasite and the human GSK-3

homologs (49% identity, 68% similarity) (supplementary Fig. 1), is far above the 30% threshold for comparative modeling. To evaluate the quality of the leishmanial GSK-3 structural model, structural comparisons were performed based on calculation of α-carbon atoms RMS deviation. The difference between our model and the aforementioned experimental structure of the *L.major* apo GSK-3 was found to be 15.51 Å, a well tolerated deviation if one considers that the corresponding difference between the indirubin complexed (2BHE) and the apo (1PW2) crystal structures of CDK2 is 16.08 Å. Furthermore, the deviation between the crystal structures of the human and the *L.major* GSK-3 homologs is even larger, at 18.6 Å. Docking experiments were performed using both structures and results (data not shown) indicated the homology model as more suitable for performing calculations.

The important residues of the leishmanial GSK-3 seem to be well conserved. The equivalent residue of $Tyr216^{hGSK\text{-}3\beta}$ that becomes phosphorylated on the activation loop is Tyr186 in the parasite GSK-3s. The catalytic residues $Asp200^{hGSK\text{-}3\beta,}$ $Glu97^{hGSK\text{-}3\beta}$ and $Lys85^{hGSK\text{-}3\beta}$ interacting with each other and with the phosphates of ATP are also conserved as $Asp170^{LGSK\text{-}3s}$, $Glu61^{LGSK\text{-}3s}$ and $Lys49^{LGSK\text{-}3s}$. The priming phosphate binding site, responsible for optimizing the orientation of primed substrates (Frame et al., 2001) for phosphorylation to occur, is formed in the leishmanial GSK-3s by Arg60, Arg150 and Lys175.

Docking calculations

The mode of interactions accommodated by the methionine gatekeeper in the leishmanial GSK-3s is dependent on the indirubin substituent and can be precisely approached only by quantum mechanical calculations. These interactions can differentiate ligand affinity in a range of 2-3 kcal/mol (Manas et al., 2004). In addition, a larger desolvation cost upon inhibitor binding should be expected in this case due to the more polar character of methionine. The entropic penalty resulting from constraining a methionine sidechain is larger than the corresponding cost for a leucine sidechain. The change of a buried leucine to a methionine has been shown experimentally to

destabilize the protein with a total entropic and desolvation cost of 1.4 kcal/mol (Lipscomb et al., 1998).

A comparison between the crystal structure of CDK2 and the homology model of CRK3 indicates three important differences in residues of the active site. $Gln131^{CDK2}$ becomes $Ala149^{CRK3}$, $Phe82^{CDK2}$ becomes $Tyr101^{CRK3}$ and $His84^{CDK2}$ becomes $Glu103^{CRK3}$. Structure refinement of the CRK3 model resulted in a conformation where the sidechains of Tyr101 and Glu103 formed a hydrogen bond (Fig. 7B). This interaction is not possible in the human CDK2 homolog. The influence of this bonding interaction on the cavity size and subsequently on the ligand affinity could explain the observed gain of selectivity of 6-BIO towards CRK3. Possibly the steric penalty resulting from the 6-substitution (Meijer et al., 2004) is counterbalanced in CRK3 by a better fit and a favorable stacking or charge dipole interaction between the aromatic system of indirubin and the Tyr101-Glu103 pair. While this is true for 6-BIO, in the case of the compounds carrying the bulkier substituents (6-IIO, 5-Me-6-BIO and 6-BIA), the presence of the additional substituent provoked a displacement of the ligand and the pair of residues Tyr101-Glu103 (Fig. 7C).

SUPPLEMENTARY REFERENCES

Ali, M.A., Choy, H., Habib, A.A., Saha, D., 2007. SNS-032 prevents tumor cell-induced angiogenesis by inhibiting vascular endothelial growth factor. Neoplasia 9, 370-381.

Coghlan, M.P., Culbert, A.A., Cross, D.A., Corcoran, S.L., Yates, J.W., Pearce, N.J., Rausch, O.L., Murphy, G.J., Carter, P.S., Roxbee Cox, L., Mills, D., Brown, M.J., Haigh, D., Ward, R.W., Smith, D.G., Murray, K.J., Reith, A.D., Holder, J.C., 2000. Selective small molecule inhibitors of glycogen synthase kinase-3 modulate glycogen metabolism and gene transcription. Chem Biol 7, 793-803.

Leost, M., Schultz, C., Link, A., Wu, Y.Z., Biernat, J., Mandelkow, E.M., Bibb, J.A., Snyder, G.L., Greengard, P., Zaharevitz, D.W., Gussio, R., Senderowicz, A.M., Sausville, E.A., Kunick, C., Meijer, L., 2000. Paullones are potent inhibitors of glycogen synthase kinase-3beta and cyclin-dependent kinase 5/p25. Eur J Biochem 267, 5983-5994.

Lipscomb, L.A., Gassner, N.C., Snow, S.D., Eldridge, A.M., Baase, W.A., Drew, D.L., Matthews, B.W., 1998. Context-dependent protein stabilization by methionine-to-leucine substitution shown in T4 lysozyme. Protein Sci 7, 765-773.

Manas, E.S., Xu, Z.B., Unwalla, R.J., Somers, W.S., 2004. Understanding the selectivity of genistein for human estrogen receptor-beta using X-ray crystallography and computational methods. Structure 12, 2197-2207.

Martinez, A., Alonso, M., Castro, A., Perez, C., Moreno, F.J., 2002. First non-ATP competitive glycogen synthase kinase 3 beta (GSK-3beta) inhibitors: thiadiazolidinones (TDZD) as potential drugs for the treatment of Alzheimer's disease. J Med Chem 45, 1292-1299.

McGovern, S.L., Shoichet, B.K., 2003. Kinase inhibitors: not just for kinases anymore. J Med Chem 46, 1478-1483.

Meijer, L., Thunnissen, A.M., White, A.W., Garnier, M., Nikolic, M., Tsai, L.H., Walter, J., Cleverley, K.E., Salinas, P.C., Wu, Y.Z., Biernat, J., Mandelkow, E.M., Kim, S.H., Pettit, G.R., 2000. Inhibition of cyclin-dependent kinases, GSK-3beta and CK1 by hymenialdisine, a marine sponge constituent. Chem Biol 7, 51-63.

Mettey, Y., Gompel, M., Thomas, V., Garnier, M., Leost, M., Ceballos-Picot, I., Noble, M., Endicott, J., Vierfond, J.M., Meijer, L., 2003. Aloisines, a new family of CDK/GSK-3 inhibitors. SAR study, crystal structure in complex with CDK2, enzyme selectivity, and cellular effects. J Med Chem 46, 222-236.

Mohamadi, F., Richards, N. G., Guida, W.C., Liskamp, R., Lipton, M., Caufield, C., Chang, G., Hendrickson, T., Still W.C., 1990. Macromodel-An integrated software system for modeling organic and bioorganic molecules using molecular mechanics. J. Comput. Chem. 11, 440-467.

SUPPLEMENTARY FIGURE LEGENDS

-Legend to supplementary Fig 1. Multiple alignment of GSK-3 from eight organisms: *L. donovani* GSK-3s (**EF620873**), *L. mexicana* GSK-3s (**Q0PKV3**), *L. major Friedlin* GSK-3s (**XP_001682433**, LmjF18.0270), *T. brucei* "short" (**Tb10.61.3140**), *H. sapiens* GSK-3β (**P49841**), *M. musculus* GSK-3β (**Q9WV60**), *D. rerio* GSK-3β (**Q1LYN4**) and *P. falciparum* (**O77344**). Numbering follows the *L. donovani* homologue. In the depiction identical residues are enclosed in black filled boxes and similar residues in black bordered boxes. Dashes indicate gaps introduced to optimize the alignment. Filled circles indicate catalytic residues (Asp 170, Glu 61, Lys 49), open circles indicate aminoacids that form the priming phosphate binding site (Arg 60, Arg 150, Lys 175). The arrow shows the "gatekeeper" residue (Met 100). Asterisks mark aminoacids located in the flexible glycine loop (Gln 28, Thr 30). The triangle highlights Tyr 186, that becomes phosphorylated on the activation loop. Alignment depiction was created with ESPript.

-Legend to supplementary Fig 2. Purity of *Ld*GSK-3s and CRK3 produced in *L. donovani* over-expressing transfectants and transgenic *L. mexicana* promastigotes respectively. The enzymes were purified by metal affinity chromatography on Ni-NTA resin as previously described. Lane 1, *Ld*GSK-3s (~41 kDa); Lane 2, CRK3 (~36 kDa). Both proteins carry a His-tag, which slightly

increases their molecular weights. Lanes were loaded with 2 μg of each protein and the purity was judged to be of approximately 95%.

-Legend to supplementary Fig 3. Lineweaver-Burke plots of the initial velocity (1/V) versus substrate concentration 1/[S], for the determination of the Km values for ATP and substrate for each kinase. A. *Ld*GSK-3s black line ATP; gray line GS-1 peptide. B. CRK3 black line ATP; gray line histone H1.

SUPPLEMENTARY TABLE

Supplementary table 1. Inhibition of *Ld*GSK-3s and CRK3 kinase activities by various inhibitors.

Compounds	**IC_{50} (μM)**	
	***Ld*GSK-3s**	**CRK3**
Kenpaullone	3	3
Alsterpaullone	0.2	0.8
Aloisine A	>10	2
Hymenialdisine	2	0.03
SB 216763	1	>10
SB 415286	0.8	>10
TDZD-8	>10	>10
SNS-032	>10	>10

supplementary figure 1

Click here to download high resolution image

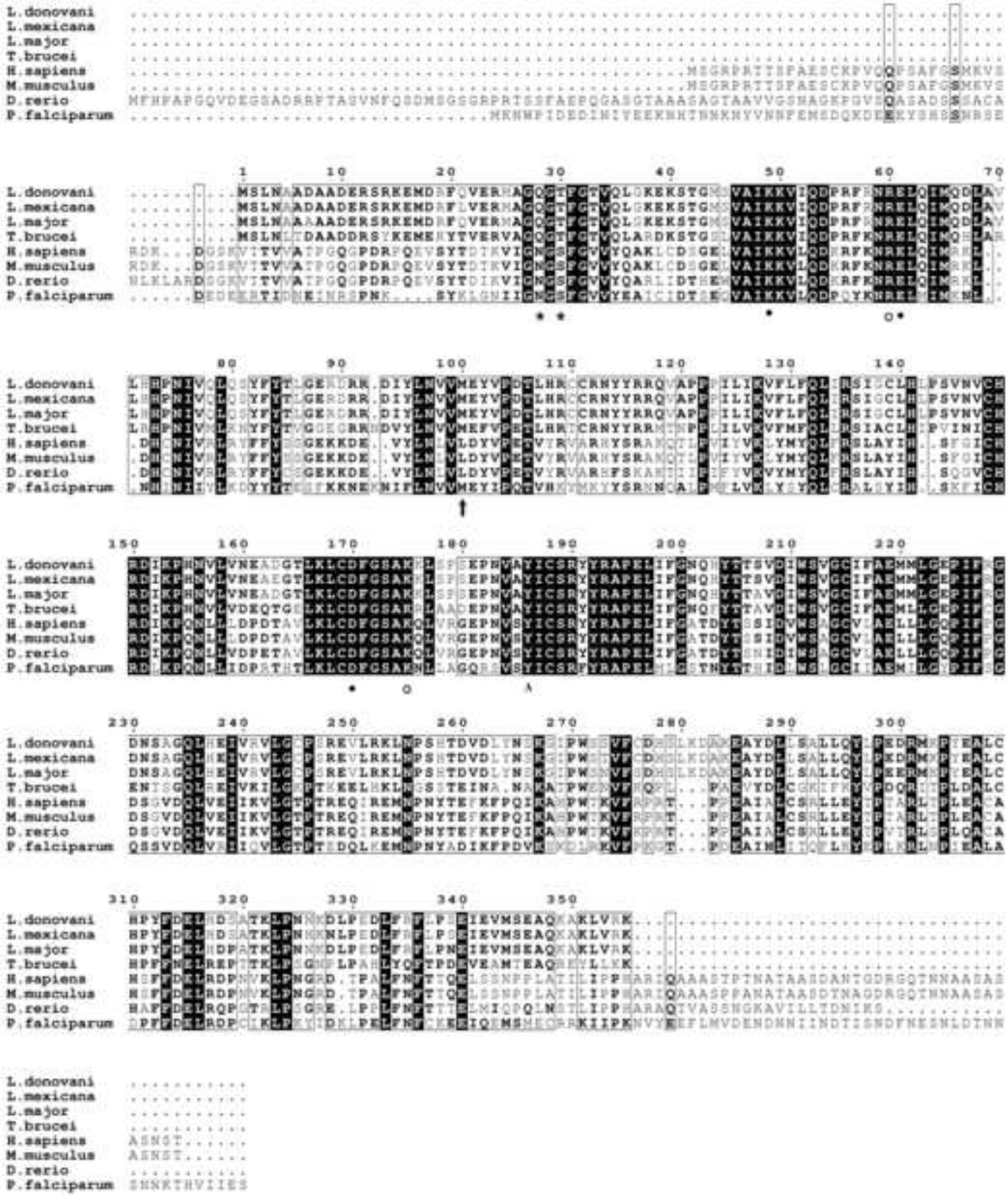

supplementary figure 2

Click here to download high resolution image

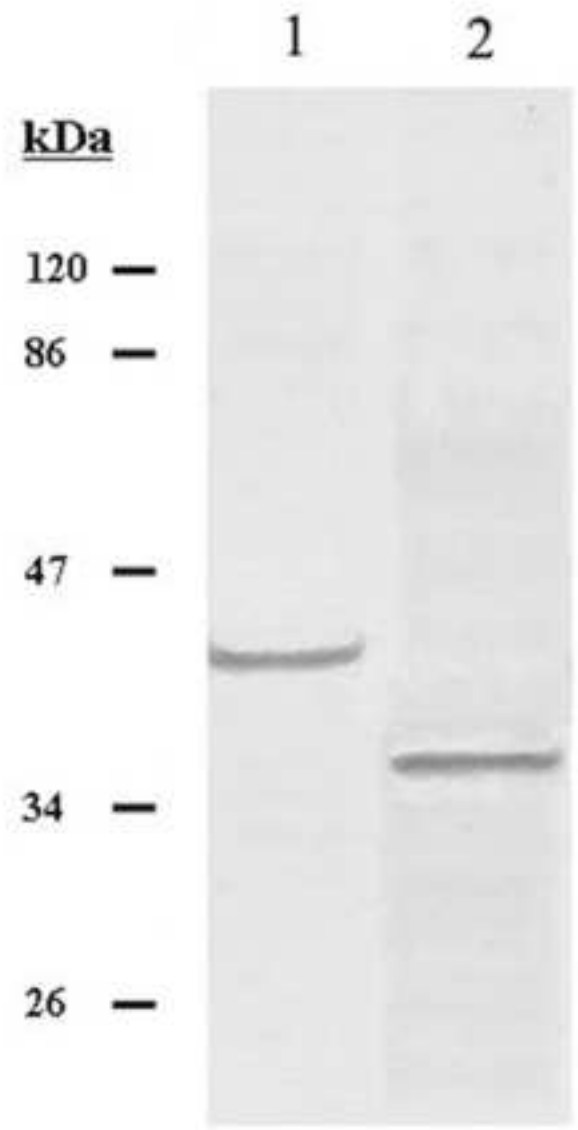

supplementary figure 3

Click here to download high resolution image